NASA/TP–2006–214141

Five Millennium Canon of Solar Eclipses: –1999 to +3000 (2000 BCE to 3000 CE)

Fred Espenak and Jean Meeus

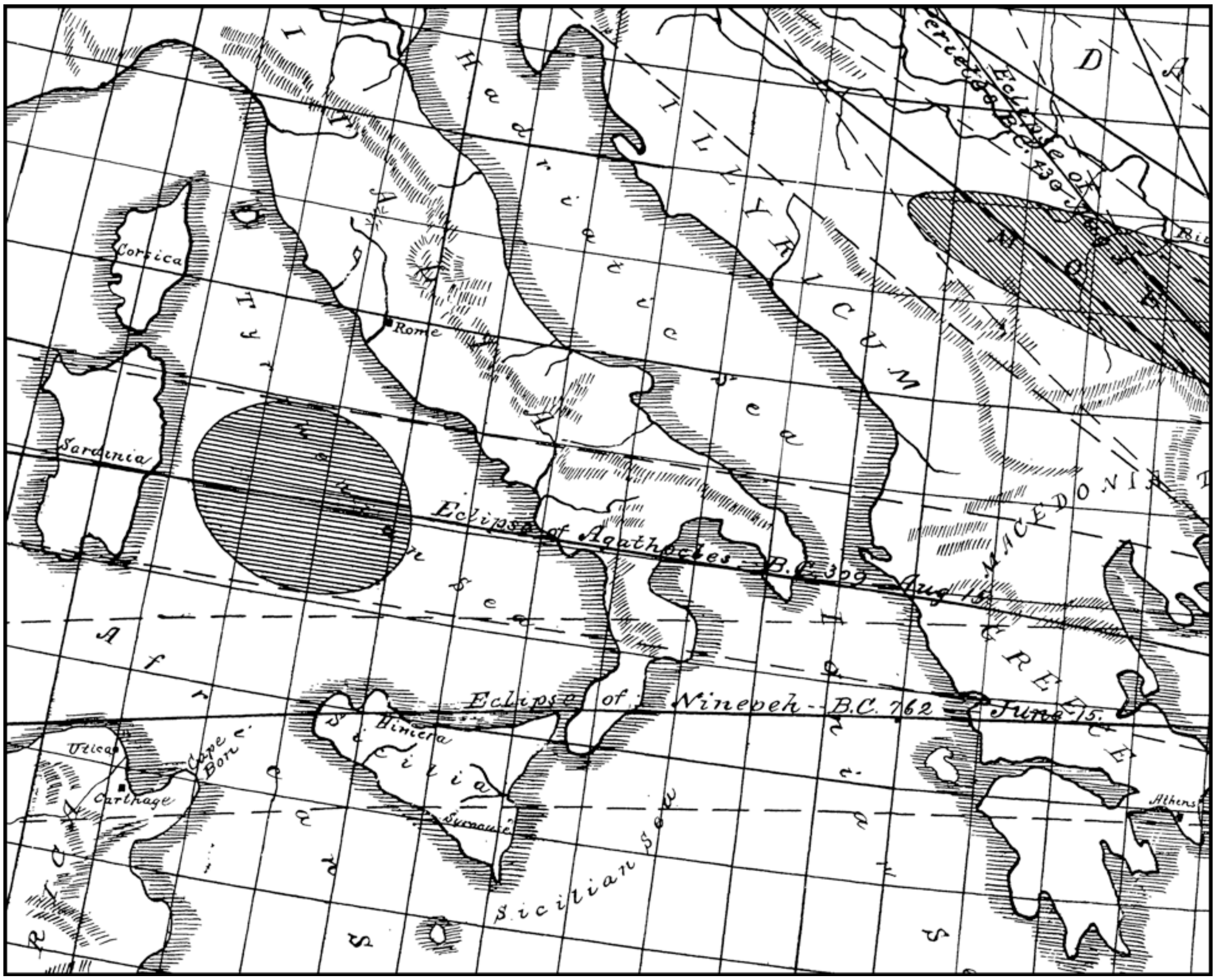

Revision 1.0 (2007 May 11)

October 2006

COVER CAPTION:

Map of ancient eclipses as drawn by John N. Stockwell in 1890.

The NASA STI Program Office … in Profile

Since its founding, NASA has been dedicated to the advancement of aeronautics and space science. The NASA Scientific and Technical Information (STI) Program Office plays a key part in helping NASA maintain this important role.

The NASA STI Program Office is operated by Langley Research Center, the lead center for NASA's scientific and technical information. The NASA STI Program Office provides access to the NASA STI Database, the largest collection of aeronautical and space science STI in the world. The Program Office is also NASA's institutional mechanism for disseminating the results of its research and development activities. These results are published by NASA in the NASA STI Report Series, which includes the following report types:

- TECHNICAL PUBLICATION. Reports of completed research or a major significant phase of research that present the results of NASA programs and include extensive data or theoretical analysis. Includes compilations of significant scientific and technical data and information deemed to be of continuing reference value. NASA's counterpart of peer-reviewed formal professional papers but has less stringent limitations on manuscript length and extent of graphic presentations.
- TECHNICAL MEMORANDUM. Scientific and technical findings that are preliminary or of specialized interest, e.g., quick release reports, working papers, and bibliographies that contain minimal annotation. Does not contain extensive analysis.
- CONTRACTOR REPORT. Scientific and technical findings by NASA-sponsored contractors and grantees.
- CONFERENCE PUBLICATION. Collected papers from scientific and technical conferences, symposia, seminars, or other meetings sponsored or cosponsored by NASA.
- SPECIAL PUBLICATION. Scientific, technical, or historical information from NASA programs, projects, and mission, often concerned with subjects having substantial public interest.
- TECHNICAL TRANSLATION. English-language translations of foreign scientific and technical material pertinent to NASA's mission.

Specialized services that complement the STI Program Office's diverse offerings include creating custom thesauri, building customized databases, organizing and publishing research results . . . even providing videos.

For more information about the NASA STI Program Office, see the following:

- Access the NASA STI Program Home Page at http://www.sti.nasa.gov/STI-homepage.html
- E-mail your question via the Internet to help@sti.nasa.gov
- Fax your question to the NASA Access Help Desk at (301) 621-0134
- Telephone the NASA Access Help Desk at (301) 621-0390
- Write to:
  NASA Access Help Desk
  NASA Center for AeroSpace Information
  7121 Standard Drive
  Hanover, MD 21076–1320

NASA/TP–2006–214141

Five Millennium Canon of Solar Eclipses: –1999 to +3000 (2000 BCE to 3000 CE)

Fred Espenak
NASA Goddard Space Flight Center, Greenbelt, Maryland

Jean Meeus (Retired)
Kortenberg, Belgium

October 2006

Available from:

NASA Center for AeroSpace Information
7121 Standard Drive
Hanover, MD 21076–1320
Price Code: A17

National Technical Information Service
5285 Port Royal Road
Springfield, VA 22161
Price Code: A10

PREFACE

Theodor von Oppolzer's 1887 *Canon der Finsternisse (Canon of Eclipses)* stands as one of the greatest accomplishments in computational astronomy of the 19th century. It contains the elements of all 8,000 solar eclipses (and 5,200 lunar eclipses) occurring between the years –1207 and +2161 (1208 BCE and 2161 CE, respectively), together with maps showing the approximate positions of the central lines. To make this remarkable achievement possible, a number of approximations were used in the calculations and maps. For instance, the central line path of each solar eclipse was computed for only three positions: sunrise, mid-point, and sunset. A circular arc was fit through the points to depict the eclipse path. Consequently, the central lines often differ by hundreds of miles compared to rigorous predictions generated with modern ephemerides. Furthermore, the 1887 Canon took no account of the shifts imparted to ancient eclipse paths as a consequence of Earth's variable rotation rate and the secular acceleration of the Moon.

Subsequently, special eclipse canons were published for shorter time intervals or for limited geographic regions. Ginzel's *Spezieller Kanon* (1899) dealt with eclipses in the period –900 to +600 (901 BCE to 600 CE), while Schroeter (1923) produced charts and data for solar eclipses visible in Europe from +600 to +1800 (600–1800 CE).

With the arrival of the electronic computer, the time was ripe to produce an updated eclipse canon. In 1966, Meeus, Grosjean, and Vanderleen published *Canon of Solar Eclipses* containing the Besselian elements of all solar eclipses from +1898 to +2510 (1898–2510 CE), together with central line tables and maps. The aim of this work was principally to provide data on future eclipses.

The next canon (Mucke and Meeus, 1983) was intended mainly for historical research and covered the period –2003 to +2526 (2004 BCE to 2526 CE). Thus, it was effectively the modern day successor of Oppolzer's great canon. The Mucke-Meeus publication included Besselian elements and maps of all 10,774 solar eclipses during this time interval. Each orthographic map was oriented to show the day-side hemisphere of Earth. In this projection, the path of the Moon's penumbra and the central axis of the shadow cone could be approximated by straight lines.

Several other special canons have been produced. Stephenson and Houlden (1986) published an atlas of annular and total eclipses visible in East Asia from –1499 to +1900 (1500 BCE to 1900 CE). Espenak's *Fifty Year Canon of Solar Eclipses* (1987) included individual detailed maps and central path data for all solar eclipses from +1986 to +2035 (1986–2035 CE).

Without exception, all solar eclipse canons produced during the latter half of the 20th century were based on Newcomb's tables of the Sun (1895) and Brown's lunar theory (1905), subject to later modifications in the *Improved Lunar Ephemeris* (1954). These were the best ephemerides of their day but they have now been superseded.

The present book contains detailed, accurate maps (found in the Appendix at the back of the book) for 5,000 years of solar eclipses, from –1999 to +3000 (2000 BCE to 3000 CE). The following points highlight the features and characteristics of this work.

- Based on modern theories of the Sun and the Moon constructed at the *Bureau des Longitudes* of Paris rather than the older Newcomb and Brown ephemerides.
- Ephemerides and eclipse predictions performed in Terrestrial Dynamical Time.
- Covers historical period of eclipses, as well as one millennium into the future.
- Global maps for each eclipse depict the actual northern and southern limits of the Moon's penumbral and umbral or antumbral shadows, as well as the sunrise and sunset curves.
- Maps include curve of eclipse magnitude 0.5.
- Maps include continental outlines with contemporary political boundaries and are large enough to identify geographic regions of eclipse visibility.

- Maps are based of the most current determination of the historical values of ΔT.
- Estimates of eclipse path accuracy based on the uncertainty in the value of ΔT (i.e., standard error in ΔT)

A primary goal of this work is to assist historians and archeologists in the identification and dating of eclipses found in references and records from antiquity. This is no easy task because there are usually several possible candidates. Accurate maps using the best available values of ΔT coupled with estimates in the standard error of ΔT, are critical in discriminating among potential eclipse candidates. Ultimately, historical eclipse identification can lead to improved chronologies in the timeline of a particular culture.

A certain synergism exists here because new eclipse identifications in the historic record can lead to new data in the determination and refinement of the historical value and behavior of ΔT. Improved values of ΔT can then lead to the positive identification of more eclipses in the historical record.

The maps can also be used to quickly estimate the approximate circumstances for any geographic location during each eclipse without any calculations. Because the northern and southern limits of total and annular eclipses are plotted, it is readily apparent by inspection whether a location is within the umbral or antumbral path. The northern and southern limits of the penumbral shadow and the curve of eclipse magnitude 0.5 can be used to estimate the magnitude of a partial eclipse. The position of the sub-solar point at greatest eclipse shows the apparent noon meridian, while the penumbra's rising and setting curves depict the regions where the eclipse is in progress during sunrise and sunset, respectively. All this can be accomplished simply by inspecting the maps.

The *Canon* will also be of value to educators, planetariums, and anyone interested in knowing when and where past and future eclipses occur. The general public is fascinated by eclipses. With each major eclipse, the question always arises as to when a particular location experienced its last and next eclipses. The maps presented here are ideally suited to addressing such queries.

Finally, if this work inspires any student to pursue a career path leading to the sciences, then we have achieved the greatest success we could possibly hope for.

—*Fred Espenak and Jean Meeus*
2006 June

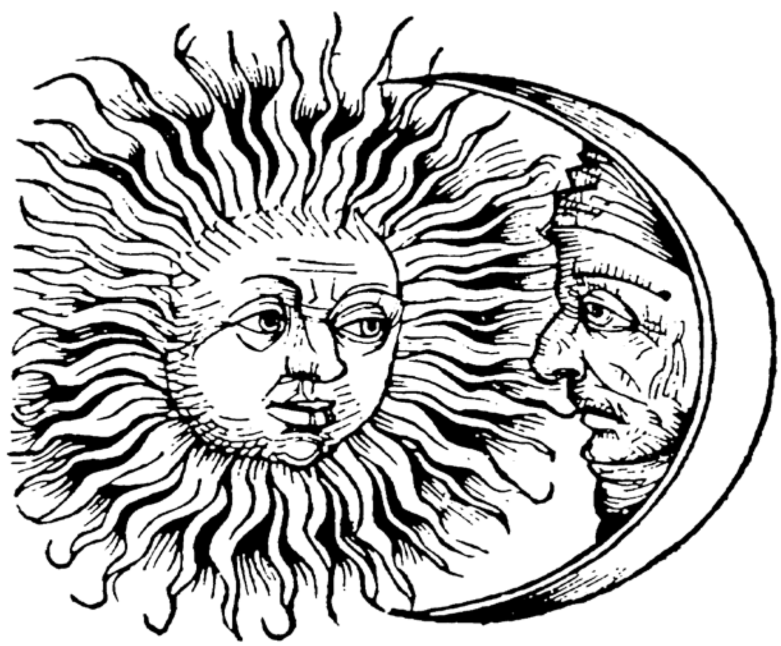

Imaginative solar eclipse from Schedel's *Nuremberg Chronicle* (1493).

TABLE OF CONTENTS

Section 1: Maps and Predictions

1.1 Introduction

Earth will experience 11,898 eclipses of the Sun during the 5000-year period from –1999 to +3000 (2000 BCE[a] to 3000 CE). An individual global map for every solar eclipse over the five millennium interval is presented in the Appendix. For partial eclipses, the path of the Moon's penumbral path depicts the geographic region of eclipse visibility. For total, hybrid, and annular eclipses, the track of the Moon's umbral/antumbral[b] shadow is also plotted. The maps include modern political borders to assist in identifying the geographic visibility of each eclipse.

1.2 Explanation of Solar Eclipse Maps

For each eclipse, an orthographic projection map of Earth shows the path of the Moon's penumbral (partial) and umbral/antumbral (total, hybrid, or annular) shadows with respect to the continental coastlines, political boundaries (circa 2000 CE), and the Equator. North is to the top, and the daylight terminator is drawn for the instant of greatest eclipse. An "x" symbol marks the sub-solar point or geographic location where the Sun appears directly overhead (zenith) at that time. All salient features of the eclipse maps are identified in Figure 1-1, which serves as a key.

Figure 1-1 - Key to Eclipse Maps

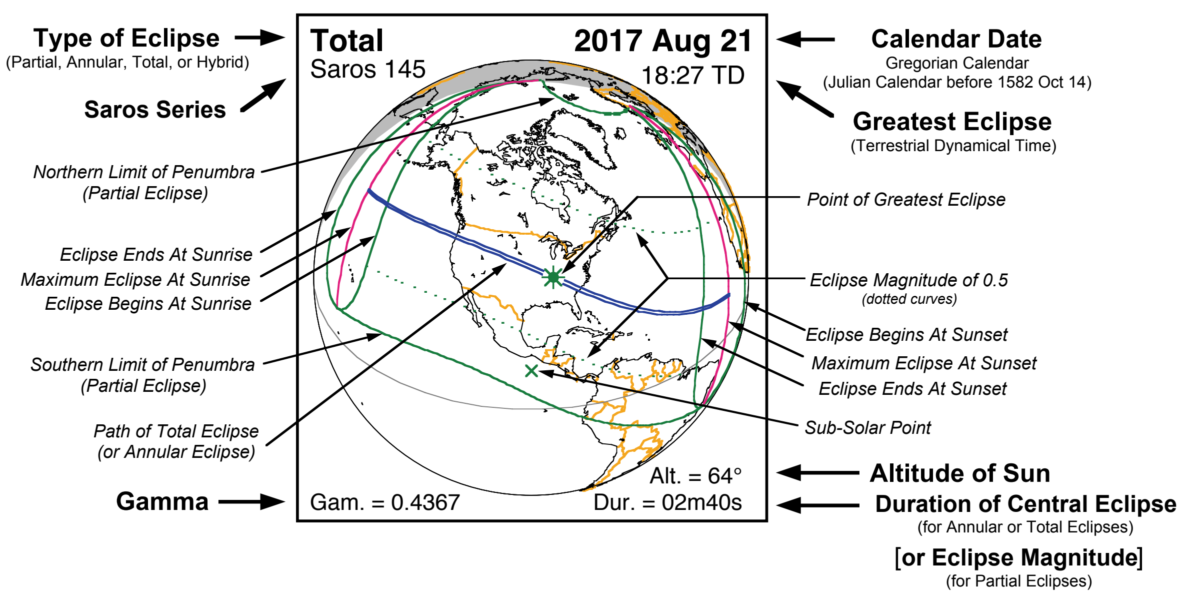

The limits of the Moon's penumbral shadow delineate the region of visibility of a partial solar eclipse. This irregular or saddle shaped region often covers more than half the daylight hemisphere of Earth and consists of several distinct zones or limits. At the northern and/or southern boundaries lie the limits of the penumbra's path. Partial eclipses have only one of these limits, as do central eclipses when the Moon's shadow axis falls no closer than about 0.45 radii from Earth's center. Great loops at the western and eastern extremes of the penumbra's path identify the areas where the eclipse begins/ends at sunrise and sunset, respectively. If the penumbra has both a northern and southern limit, the rising and setting curves form two separate, closed loops (e.g., 2017 Aug 21). Otherwise, the curves are connected in a distorted figure eight (e.g., 2019 Jul 02). Bisecting the "eclipse begins/ends at sunrise and sunset" loops is the curve of maximum eclipse at sunrise (western loop) and sunset (eastern loop).

a. The terms BCE and CE are abbreviations for "Before the Common Era" and "Common Era," respectively. They are the secular equivalents to the BC and AD dating conventions. A major advantage of the BCE/CE convention is that both terms are suffixes, whereas BC and AD are used as a suffix and prefix, respectively.

b. The term "umbral/antumbral" means "umbral and/or antumbral."

The eclipse magnitude is defined as the fraction of the Sun's diameter occulted by the Moon. The curves of eclipse magnitude 0.5 delineate the locus of all points where the local magnitude at maximum eclipse is equal to 0.5. These curves run exclusively between the curves of maximum eclipse at sunrise and sunset. They are approximately parallel to the northern/southern penumbral limits and the umbral/antumbral paths of central eclipses. The northern and southern limits of the penumbra may be thought of as curves of eclipse magnitude of 0.0. For total eclipses, the northern and southern limits of the umbra are curves of eclipse magnitude of 1.0.

Greatest eclipse is the instant when the axis of the Moon's shadow cone passes closest to Earth's center. Although greatest eclipse differs slightly from the instants of greatest magnitude and greatest duration (for total eclipses), the differences are negligible. The point on Earth's surface intersected by the axis of the Moon's shadow cone at greatest eclipse is marked by an asterisk symbol "*". For partial eclipses, the shadow axis misses Earth entirely, so the point of greatest eclipse lies on the day/night terminator and the Sun appears on the horizon.

Data relevant to an eclipse appear in the corners of each map. In the top left corner are the eclipse type (total, hybrid, annular, or partial) and the Saros series of the eclipse. To the top right are the Gregorian calendar date (Julian calendar prior to 1582 Oct 14) and the time of greatest eclipse (Terrestrial Dynamical Time). The bottom left corner lists gamma, the minimum distance of the axis of the Moon's shadow cone from Earth's center (in Earth equatorial radii). The Sun's altitude at the geographic position of greatest eclipse is found to the lower right. The content of the final datum depends on the type of eclipse. If the eclipse is partial then the eclipse magnitude is given. If the eclipse is total, hybrid, or annular, then the duration of the total or annular phase is given at the position and instant of greatest eclipse. A detailed explanation of each of these items appears in the following sections.

1.2.1 Eclipse Type

There are four basic types of solar eclipses:

1) Partial—Moon's penumbral shadow traverses Earth (umbral/antumbral shadow completely misses Earth)
2) Annular—Moon's antumbral[a] shadow traverses Earth (the Moon is too far from Earth to completely cover the Sun)
3) Total—Moon's umbral shadow traverses Earth (Moon is close enough to Earth to completely cover the Sun)
4) Hybrid—Moon's umbral and antumbral shadows traverse different parts of Earth (eclipse appears either total or annular along different sections of its path). Hybrid eclipses are also known as annular-total eclipses.

1.2.2 Saros Series Number

Each eclipse belongs to a Saros series (Sect. 4.2) using a numbering system first introduced by van den Bergh (1955). This system has been expanded to include negative values from the past, as well as additional series in the future. The eclipses with an odd Saros number take place at the ascending node of the Moon's orbit; those with an even Saros number take place at the descending node.

The Saros is a period of 223 synodic months, or approximately 18 years, 11 days, and 8 hours. Eclipses separated by this period belong to the same Saros series and share very similar geometry and characteristics.

---

a. The cone-shaped umbra gradually narrows to a point. Beyond this vertex, an inverted cone is formed by extending the sides of the umbra. This zone is known as the antumbra. It corresponds to the region in the Moon's shadow where the Moon appears smaller than the Sun. The Moon is then seen in complete silhouette against the Sun's photospheric disk.

1.2.3 Calendar Date

All eclipse dates from 1582 Oct 15 onwards use the modern Gregorian calendar currently found throughout most of the world. The older Julian calendar is used for eclipse dates prior to 1582 Oct 04. Because of the Gregorian Calendar Reform, the day following 1582 Oct 04 (Julian calendar) is 1582 Oct 15 (Gregorian calendar).

The Gregorian calendar was decreed by Pope Gregory XIII in 1582 to correct a problem in a drift of the seasons. It adopts the convention of a year containing 365 days. Every fourth year is a leap year of 366 days if it is divisible by 4 (e.g., 2004, 2008, etc.). However, whole century years (e.g., 1700, 1800, 1900) are excluded from the leap year rule unless they are also divisible by 400 (e.g., 2000). This complicated dating scheme was designed to keep the vernal equinox on or within a day of March 21.

Prior to the Gregorian Calendar Reform in 1582, the Julian calendar was in wide use. It was simpler than the Gregorian in that all years divisible by 4 were counted as 366-day leap years. This simplicity came at a cost. After more than 16 centuries of use, the Julian calendar date of the vernal equinox had drifted 11 days from March 21. It was this failure of the Julian calendar that resulted in the Gregorian Calendar Reform.

The Julian calendar does not include the year 0, so the year 1 BCE is followed by the year 1 CE. This is awkward for arithmetic calculations. In this publication, dates are counted using the astronomical numbering system which recognizes the year 0. Historians should note the numerical difference of one year between astronomical dates and BCE dates. Thus, the year 0 corresponds to 1 BCE, and the year –100 corresponds to 101 BCE, etc.

There are a number of ways to write the calendar date through variations in the order of day, month, and year. The International Organization for Standardization's (ISO) 8601 advises a numeric date representation, which organizes the elements from the largest to the smallest. The exact format is YYYY-MM-DD where YYYY is the calendar year, MM is the month of the year between 01 (January) and 12 (December), and DD is the day of the month between 01 and 31. For example, the 27th day of April in the year 1943 would then be expressed as 1943-04-27. We support the ISO convention, but have replaced the month number with the three-letter English abbreviation of the month name for additional clarity. From the previous example, we express the date as 1943 Apr 27.

1.2.4 Greatest Eclipse

The instant of greatest eclipse occurs when the distance between the axis of the Moon's shadow cone and the center of Earth reaches a minimum. For partial eclipses, the instant of greatest eclipse differs slightly from the instant of greatest magnitude primarily because of Earth's flattening. For total eclipses, the instant of greatest eclipse differs slightly from the instant of greatest duration, although the differences are quite small.

Solar eclipses occur when the Moon is near one of the nodes of its orbit, and therefore, moving at an angle of about 5° to the ecliptic. Hence, unless the eclipse is perfectly central, the instant of greatest eclipse does not coincide with that of apparent ecliptic conjunction (i.e., New Moon), nor with the time of conjunction in Right Ascension.

Greatest eclipse is given in Terrestrial Dynamical Time (TD, Sect. 2.3), which is a time system based on International Atomic Time. As such TD is the atomic time equivalent to its predecessor Ephemeris Time (Sect. 2.2) and is used in the theories of motion for bodies in the Solar System. To determine the geographic visibility of an eclipse, TD is converted to Universal Time (Sect. 2.4) using the parameter ΔT (Sects. 2.6 and 2.7).

1.2.5 Gamma

The quantity gamma is the minimum distance from the axis of the lunar shadow cone to the center of Earth, in units of Earth's equatorial radius. This distance is positive or negative, depending on whether the axis of the shadow cone passes north or south of Earth's center. If gamma is between +0.997 and –0.997, the eclipse is a central one (either total, annular, or hybrid). The limiting value 0.997 differs from unity because of the flattening of Earth.

The change in the value of gamma, after one Saros period, is larger when Earth is near its aphelion (June–July) than when it is near perihelion (December–January). Table 1-1 illustrates this point using eclipses from two different Saros series.

Table 1-1. Variation in Gamma at Aphelion vs. Perihelion

Date	Gamma	Date	Gamma
1955 Jun 20	–0.15278	1956 Dec 02	+1.09229
1973 Jun 30	–0.07853	1974 Dec 13	+1.07975
1991 Jul 11	–0.00412	1992 Dec 24	+1.07107
2009 Jul 22	+0.06977	2011 Jan 04	+1.06265
2027 Aug 02	+0.14209	2029 Jan 14	+1.05532

A similar situation exists in the case of lunar eclipses. The explanation can be found in van den Bergh (1955).

1.2.6 Altitude of Sun

The Sun's altitude at the geographic position intersected by the axis of the lunar shadow cone is given at the instant of greatest eclipse. For partial eclipses, the Sun's altitude is always 0° because the shadow axis misses Earth. In this case, the geographic position corresponds to the point closest to the shadow axis.

1.2.7 Duration of Central Eclipse

For central eclipses (total, annular, or hybrid), the duration of the total or annular phase (in minutes and seconds) is given at the geographic position intersected by the axis of the lunar shadow cone at the instant of greatest eclipse.

In the case of a total or hybrid eclipse, this duration is very nearly, but not exactly, the maximum duration of the total phase along the entire umbral path. For an annular eclipse, the duration at greatest eclipse may be near either the minimum or maximum duration of the annular phase along the path. If the annular phase duration exceeds approximately 2.3 min, then it corresponds to the near maximum duration along the central line track. If the annular phase duration is less, however, then it corresponds to a near minimum and the annular duration increases towards the ends of the central path.

1.2.8 Eclipse Magnitude

The eclipse magnitude is defined as the fraction of the Sun's diameter occulted by the Moon. For partial eclipses, the eclipse magnitude at the instant of greatest eclipse is given for the geographic position closest to the axis of the Moon's shadow cone. The eclipse magnitude is always less than 1.0 for partial and annular eclipses, but equal to or greater than 1.0 for total and hybrid eclipses.

1.2.8 Additional Elements

Two additional parameters are listed at the bottom of each map page. The first element is ΔT (Sect. 2.6). It is the arithmetic difference between TD (Sect. 2.3) and Universal Time (Sect. 2.4). The value given is specific to the first eclipse on the page. Next to ΔT is its corresponding standard error. This is the estimated uncertainty in ΔT (Sect. 2.8) and is given both in seconds, and in the equivalent shift in longitude east or west.

1.3 Solar and Lunar Coordinates

The coordinates of the Sun used in these eclipse predictions have been calculated on the basis of the VSOP87 theory constructed by Bretagnon and Francou (1988) at the *Bureau des Longitudes,* Paris. This theory gives the ecliptic longitude and latitude of the planets, and their radius vector, as sums of periodic terms. In our calculations, we used the complete set of periodic terms of version D of VSOP87 (this version provides the positions referred to the mean equinox of the date).

For the Moon, use has been made of the theory ELP-2000/82 of Chapront-Touzé and Chapront (1983), again of the *Bureau des Longitudes.* This theory contains a total of 37,862 periodic terms, namely 20,560 for the Moon's longitude, 7,684 for the latitude, and 9,618 for the distance to Earth. But many of these terms are very small: some have an amplitude of only 0.00001 arcsec for the longitude or the latitude, and of 2 cm for the distance. In our computer program, we neglected all periodic terms with coefficients smaller than 0.0005 arcsec in longitude and latitude, and smaller than 1 m in distance. Because of neglecting the very small periodic terms, the Moon's positions calculated in our program have a mean error (as compared to the full ELP theory) of about 0.0006 s of time in right ascension, and about 0.006 arcsec in declination. The corresponding error in the calculated times of the phases of a solar eclipse is of the order of 1/40 s, which is much smaller than the uncertainties in predicted values of ΔT, and also much smaller than the error due to neglecting the irregularities (mountains and valleys) at the lunar limb.

Improved expressions for the mean arguments L′, D, M, M′, and F have been taken from Chapront, Chapront-Touzé, and Francou (2002). A major consequence of this work is to bring the secular acceleration of the Moon's longitude (–25.858 arcsec/cy^2, where arcsec/cy^2 is arc seconds per Julian century squared[a]) into good agreement with Lunar Laser Ranging (LLR) observations from 1972 to 2001 (Sect. 1.4).

The center of figure of the Moon does not coincide exactly with its center of mass. To compensate for this property in their eclipse predictions, many of the national institutes employ an empirical correction to the center of mass position of the Moon. This correction is typically +0.50 arcsec in longitude and –0.25 arcsec in latitude. Unfortunately, the large variation in lunar libration from one eclipse to the next minimizes the effectiveness of the empirical correction. We choose to ignore this convention and have performed all calculations using the Moon's center of mass position. In any case, it has no practical impact on the present work.

1.4 Secular Acceleration of the Moon

Ocean tides are caused by the gravitational pull of the Moon (and, to a lesser extent, the Sun). The resulting tidal bulge in Earth's oceans is dragged ahead of the Moon in its orbit because of the daily rotation of Earth. As a consequence, the ocean mass offset from the Earth–Moon line exerts a pull on the Moon and accelerates it in its orbit. Conversely, the Moon's gravitational tug on this mass exerts a torque that decelerates the rotation of Earth. The length of the day gradually increases as energy is transferred from Earth to the Moon, causing the lunar orbit and period of revolution about Earth to increase.

This secular acceleration of the Moon is small, but it has a cumulative effect on the Moon's position when extrapolated over many centuries. Direct measurements of the acceleration have only been possible since 1969 using the Apollo retro-reflectors left on the Moon. The results from LLR show that the Moon's mean distance from Earth is increasing by 3.8 cm per year (Dickey, et al., 1994). The corresponding acceleration in the Moon's ecliptic longitude is –25.858 arcsec/cy^2 (Chapront, Chapront-Touzé, and Francou, 2002). This is the value we have adopted in our lunar ephemeris calculations.

a. This unit, arcsec/cy^2, is used in discussing secular changes in the Moon's longitude over long time intervals.

There is a close correlation between the Moon's secular acceleration and changes in the length of the day. The relationship, however, is not exact because the lunar orbit is inclined anywhere from about 18.5° to 28.5° to Earth's equator. The parameter ΔT (Sects. 2.6 and 2.7) is a measure of the accumulated difference in time between an ideal clock and one based on Earth's rotation as it gradually slows down. Published determinations of ΔT from historical eclipse records have assumed a secular acceleration of –26 arcsec/cy^2 (Morrison and Stephenson, 2004). Because we have adopted a slightly different value for the secular acceleration, we must make a small correction "*c*" to the published values of ΔT as follows:

$$c = -0.91072\ (-25.858 + 26.0\ )\ u^2, \tag{1}$$

where u = (year –1955)/100.

Then

$$\Delta T\ (\text{corrected}) = \Delta T + c. \tag{2}$$

Evaluation of the correction at 1,000 year intervals over the period spanned by the *Canon* is found in Table 1-2.

Table 1-2. Corrections to ΔT Due to Secular Acceleration

Year	Correction (seconds)
–2000	–202
–1000	–113
0	–49
+1000	–12
+2000	0
+3000	–14

The correction is only important for negative years, although it is significantly smaller than the actual uncertainty in ΔT itself (Sect. 2.8).

The secular acceleration of the Moon is very poorly known and may not be constant. Careful records for its derivation only go back about a century. Before then, spurious and often incomplete eclipse and occultation observations from medieval and ancient manuscripts comprise the database. In any case, the current value implies an increase in the length of day (LOD) of about 2.3 milliseconds per century. Such a small amount may seem insignificant, but it has very measurable cumulative effects. At this rate, time as measured through Earth's rotation is losing about 84 seconds per century squared when compared to atomic time.

1.5 Mean Lunar Radius

A fundamental parameter used in eclipse predictions is the Moon's radius, *k*, expressed in units of Earth's equatorial radius. The Moon's actual radius varies as a function of position angle and libration because of irregularity in the limb profile. From 1968 to 1980, the Nautical Almanac Office used two separate values for *k* in their predictions. The larger value (*k*=0.2724880), representing a mean over topographic features, was used for all penumbral (exterior) contacts and for annular eclipses. A smaller value (*k*=0.272281), representing a mean minimum radius, was reserved exclusively for umbral (interior) contact calculations of total eclipses (*Explanatory Supplement*, 1974). Unfortunately, the use of two different values of *k* for total and annular eclipses introduces a discontinuity in the case of hybrid eclipses.

In 1982, the International Astronomical Union (IAU) adopted a value of k=0.2725076 for the lunar radius, based on a mean including mountain peaks and valleys along the Moon's limb. This value is currently used by the Nautical Almanac Office for all solar eclipse predictions. The adoption of one single value for k eliminates the discontinuity in the case of hybrid eclipses and ends confusion arising from the use of two different values. However, the use of even the best mean value for the Moon's radius introduces a problem in predicting the true character and duration of umbral and antumbral eclipses, particularly total eclipses. A total eclipse can be defined as an eclipse in which the Sun's disk is completely occulted by the Moon. This cannot occur so long as any photospheric rays are visible through deep valleys along the Moon's limb (Meeus, Grosjean, and Vanderleen, 1966); but the use of the IAU's mean k guarantees that some annular or hybrid eclipses will be misidentified as total. A case in point is the eclipse of 1986 Oct 03. Using the IAU value for k, the *Astronomical Almanac* identified this event as a total eclipse of 3 s duration when it was, in fact, a beaded annular eclipse. Because a smaller value of k is more representative of the deeper lunar valleys and hence, the minimum solid disk radius, it helps ensure the correct identification of an eclipse's actual type.

This publication adopts the two values for k used by the Nautical Almanac Office from 1968 through 1980. The larger value (k=0.2724880) is utilized for all partial (penumbral) eclipses. The magnitudes of these eclipses typically agree to within 0.0001 of the magnitudes calculated using the IAU value for k.

In order to avoid eclipse type misidentification and to predict central durations, which are closer to the actual durations at total eclipses, the smaller value (k=0.272281) is used for all umbral and antumbral eclipses (total, annular, and hybrid). This usage of the smaller k value is consistent with predictions in *Fifty Year Canon of Solar Eclipses: 1986–2035* (Espenak, 1987). Consequently, the smaller k produces shorter central durations and narrower paths for total eclipses when compared with calculations using the IAU value for k. Similarly, predictions using the smaller k result in longer central durations and wider paths for annular eclipses than do predictions using the IAU's k.

1.6 Map Accuracy

The accuracy of the eclipse maps depends principally on two factors. The first is the rigorousness of the solar and lunar ephemerides used in the calculations (Sect. 1.3). The Moon's close proximity to Earth coupled with its relatively low mass, results in orbital perturbations that make the Moon's position far more difficult to predict compared to the Sun's position. Nevertheless, the lunar ephemeris is accurate to better than an arcsecond within several centuries of the present. Even for eclipses occurring in the year –1999 (2000 BCE), the Moon's position is correct to within a small fraction of a degree. Such positional discrepancies correspond to errors in predicted eclipse paths that are below the resolution threshold of the maps presented in the *Canon*.

A far greater source of error in the geographic position of eclipse paths is due to the uncertainty in ΔT (Sect. 2.6). This parameter is the arithmetic difference between TD (Sect. 2.3) and Universal Time or UT (Sect. 2.4). TD can be thought of as time measured with an idealized or perfect clock. In contrast, UT is based on Earth's rotation, which is gradually slowing down. TD is used to calculate solar system ephemerides and eclipse predictions, but UT is used for defining world time and longitudes.

Earth was rotating faster in the past so eclipse predictions generated in TD must first be converted to UT (via ΔT) before the geographic path of the Moon's shadow can be determined. In other words, the physical impact of ΔT on eclipse predictions is to shift the eclipse path east relative to the position calculated from TD. Because 1° in longitude corresponds to 4 min of time, a ΔT value of 240 s would shift the eclipse path 1° east of its TD position. The maps in the *Canon* already include the ΔT translation of eclipse paths from TD to UT; thus, they depict the actual geographic regions of visibility of each eclipse.

The problem with ΔT is that it is an observationally determined quantity. In the distant past or future, the value of ΔT must be estimated from historical trends. The further removed such evaluations are from actual measurements, the greater the probable error in the extrapolated value of ΔT. Small deviations can quickly propagate into large uncertainties over the course of 1,000 years.

At the bottom of each map page is the value of ΔT and its corresponding standard error. This is an estimate of the uncertainty in the longitude determination of each map. For years in which the standard error is greater than 265 s (1.1° in longitude), the maps include a reference gore to graphically depict the longitudinal range of solutions within the standard error. The years prior to +0001 and after +2300 have uncertainties of this magnitude or greater.

The meridian representing the nominal value of ΔT is plotted as a circle of longitude running vertically through the center of each map. The reference gore then takes the form of two dashed circles of longitude east and west of the nominal ΔT meridian. They indicate the range of uncertainty in the position of the nominal ΔT meridian given the standard error (σ) in ΔT (i.e., ΔT ± σ). This means that the entire map beneath the eclipse path can be rotated east or west by this amount to produce an acceptable solution that falls within the standard error of the estimated value of ΔT.

Figure 1-2a identifies the components of the reference gore for the total solar eclipse of –1996 Oct 04 (1997 BCE). The instant of greatest eclipse is 23:24 TD (upper right corner) and the estimated value of ΔT (bottom) is 46,358 s or 12 h 53 min. The time expressed in UT is then:

$$UT = TD - \Delta T = 23{:}24 - 12{:}53 = 10{:}31 \text{ UT}. \qquad (3)$$

The time in UT is needed to determine the shift of the eclipse path relative to its TD position. The result shows the geographic region of eclipse visibility (Fig. 1-2a), taking into account the fact that Earth rotated faster 4,000 years ago. In Fig. 1-2a, the nominal ΔT meridian is identified as "ΔT", while the eastern and western reference gore longitudes are labeled "ΔT_1" (= ΔT + σ) and "ΔT_2" (= ΔT – σ), respectively. These circles of longitude are located ± 15.5° (σ = ±3,712 s) with respect to the nominal ΔT meridian and show the range that the underlying map can be rotated to give a solution, given the uncertainty in ΔT.

The map in Figure 1-2b shows the solution when ΔT_1 (= ΔT + σ) is used to calculate UT. In this case, ΔT_1 is equal to ΔT plus the standard error:

$$\Delta T_1 = \Delta T + \sigma = 46{,}358 \text{ s} + 3712 \text{ s} = 50{,}070 \text{ s} = 13\text{h } 54\text{m}. \qquad (4)$$

The corresponding time in UT is then

$$UT = TD - \Delta T = 23{:}24 - 13{:}54 = 09{:}30 \text{ UT}. \qquad (5)$$

The global map shows that entire eclipse path is shifted 15.5° east of the nominal solution for ΔT = 46,358 s.

Finally, the map in Fig. 1-2c shows the solution when ΔT_2 (= ΔT – σ) is used to calculate UT. In this case, ΔT_2 is equal to ΔT minus the standard error:

$$\Delta T_2 = \Delta T - \sigma = 46{,}358 \text{ s} - 3{,}712 \text{ s} = 42{,}646 \text{ s} = 11\text{h } 51\text{m}. \qquad (6)$$

The corresponding time in UT is then

$$UT = TD - \Delta T = 23{:}24 - 11{:}51 = 11{:}33 \text{ UT}. \qquad (7)$$

The global map shows that the entire eclipse path is now shifted 15.5° west of the nominal solution for ΔT = 46,358 s.

The reference gores plotted on eclipse maps prior to the year +0001 and after the year +2300 can be used to estimate the range of uncertainty in the geographic visibility of an eclipse given the standard error in the corresponding value of ΔT.

Fig. 1-2a

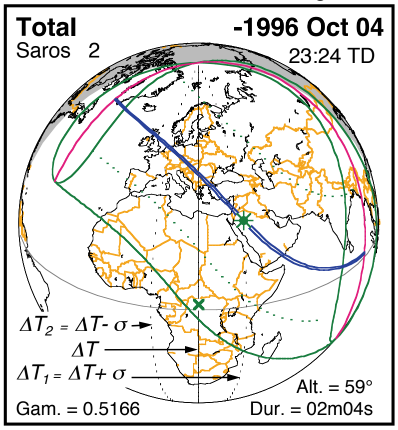

ΔT = 46358 s [= 12h53m] **10:31 UT**
std.err. (σ) = ± 3712 s [= ± 15.5°]

Fig. 1-2b

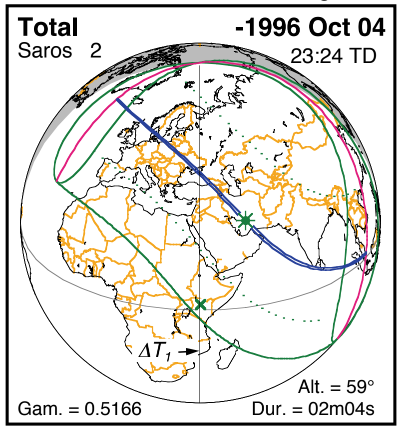

ΔT_1 = 50070 s [= 13h54m] **09:30 UT**
($\Delta T_1 = \Delta T + \sigma = 46358 + 3712$)

Fig. 1-2c

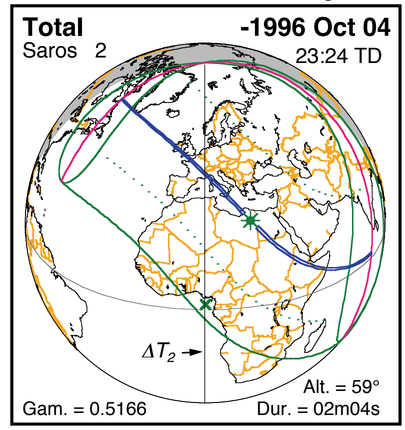

ΔT_2 = 42646 s [= 11h51m] **11:33 UT**
($\Delta T_2 = \Delta T - \sigma = 46358 - 3712$)

1.7 Eclipse Catalog

A catalog listing basic details about each eclipse in the *Canon* is available online at:

http://sunearth.gsfc.nasa.gov/eclipse/SEcat5/catalog.html

All the information found on the maps is included (calendar date, Dynamical Time, eclipse type, Saros number, gamma, altitude, and magnitude or duration). In addition, a number of other useful data are listed including ΔT, the geographic coordinates of greatest eclipse and the path width for umbral/antumbral eclipses. The eclipse type is augmented to indicate the first/last eclipse in a Saros series, umbral/antumbral eclipses with one limit, and non-central eclipses.

Section 2: Time

2.1 Greenwich Mean Time

For thousands of years, time has been measured using the length of the solar day. This is the interval between two successive returns of the Sun to an observer's local meridian. Unfortunately, the length of the apparent solar day can vary by tens of seconds over the course of a year. Earth's elliptical orbit around the Sun and the 23.5° inclination of Earth's axis of rotation are responsible for these variations. Apparent solar time was eventually replaced by mean solar time because it provides for a uniform time scale. The key to mean solar time is the mean solar day, which has a constant length of 24 hours throughout the year.

Mean solar time on the 0° longitude meridian in Greenwich, England is known as Greenwich Mean Time (GMT). At the International Meridian Conference of 1884, GMT[a] was adopted as the reference time for all clocks around the world. It was also agreed that all longitudes would be measured east or west with respect to the Greenwich meridian. In 1972, GMT was replaced by Coordinated Universal Time (UTC) as the international time reference. Nevertheless, UTC is colloquially referred to as GMT although this is technically not correct.

2.2 Ephemeris Time

During the 20th century, it was found that the rotational period of Earth (length of the day) was gradually slowing down. For the purposes of orbital calculations, time using Earth's rotation was abandoned for a more uniform time scale based on Earth's orbit about the Sun. In 1952, the International Astronomical Union (IAU) introduced Ephemeris Time to address this problem. The ephemeris second was defined as a fraction of the tropical year for 1900 Jan 01 as calculated from Newcomb's tables of the Sun (1895). Ephemeris Time was used for Solar System ephemeris calculations until it was replaced by TD in 1979.

2.3 Terrestrial Dynamical Time

TD was introduced by the IAU in 1979 as the coordinate time scale for an observer on the surface of Earth. It takes into account relativistic effects and is based on International Atomic Time (TAI) which is a high-precision standard using several hundred atomic clocks worldwide. As such TD is the atomic time equivalent to its predecessor Ephemeris Time (ET) and is used in the theories of motion for bodies in the Solar System. To ensure continuity with Ephemeris Time, TD was defined to match ET for the date 1977 Jan 01. In 1991, the IAU refined the definition of TD to make it more precise. It was also renamed Terrestrial Time (TT), although we prefer, and use, the older name Terrestrial Dynamical Time.

2.4 Universal Time

For many centuries, the fundamental unit of time was the rotational period of Earth with respect to the Sun. GMT was the standard time reference based on the mean solar time on the 0° longitude meridian in Greenwich, England. Universal Time (UT) is the modern counterpart to GMT and is determined from Very Long Baseline Interferometry (VLBI) observations of the diurnal motion of quasars. Unfortunately, Universal Time is not a uniform time scale because Earth's rotational period is (on average) gradually increasing.

---

a. GMT was originally reckoned from noon to noon. In 1925, some countries shifted GMT by 12 h so that it would begin at Greenwich midnight. This new definition is the one in common usage for world time and in the navigational publications of English-speaking countries. The designation Greenwich Mean Astronomical Time (GMAT) is reserved for the reckoning of time from noon (and previously called GMT).

The change is primarily due to tidal friction between Earth's oceans and its rocky mantle through the gravitational attraction of the Moon and, to a lesser extent, the Sun. This secular acceleration (Sect. 1.4) gradually transfers angular momentum from Earth to the Moon. As Earth loses energy and slows down, the Moon gains this energy and its orbital period and distance from Earth increase. Shorter period fluctuations in terrestrial rotation also exist, which can produce an accumulated clock error of ±20 s in one or more decades. These decade variations are attributed to several geophysical mechanisms including fluid interactions between the core and mantle of Earth. Climatological changes and variations in sea-level may also play significant roles since they alter Earth's moment of inertia.

The secular acceleration of the Moon implies an increase in the length of day (LOD) of about 2.3 milliseconds per century. Such a small amount may seem insignificant, but it has very measurable cumulative effects. At this rate, time as measured through Earth's rotation is losing about 84 seconds per century squared when compared to atomic time.

2.5 Coordinated Universal Time

Coordinated Universal Time (UTC) is the present day basis of all civilian time throughout the world. Derived from TAI, the length of the UTC second is defined in terms of an atomic transition of the element cesium and is accurate to approximately 1 ns (billionth of a second) per day. Because most daily life is still organized around the solar day, UTC was defined to closely parallel Universal Time. The two time systems are intrinsically incompatible, however, because UTC is uniform while UT is based on Earth's rotation, which is gradually slowing. In order to keep the two times within 0.9 s of each other, a leap second is added to UTC about once every 12 to 18 months.

2.6 Delta T (ΔT)

The orbital positions of the Sun and Moon required by eclipse predictions, are calculated using TD because it is a uniform time scale. World time zones and daily life, however, are based on UT[a]. In order to convert eclipse predictions from TD to UT, the difference between these two time scales must be known. The parameter delta-T (ΔT) is the arithmetic difference, in seconds, between the two as:

$$\Delta T = TD - UT. \tag{8}$$

Past values of ΔT can be deduced from the historical records. In particular, hundreds of eclipse observations (both solar and lunar) were recorded in early European, Middle Eastern, and Chinese annals, manuscripts, and canons. In spite of their relatively low precision, these data represent the only evidence for the value of ΔT prior to 1600 CE. In the centuries following the introduction of the telescope (circa 1609 CE), thousands of high quality observations have been made of lunar occultations of stars. The number and accuracy of these timings increase from the 17th through the 20th century, affording valuable data in the determination of ΔT. A detailed analysis of these measurements fitted with cubic splines for ΔT from –500 to +1950 is presented in Table 2-1 and includes the standard error for each value (Morrison and Stephenson, 2004).

a. World time zones are actually based on UTC. It is an atomic time synchronized and adjusted to stay within 0.9 s of astronomically determined UT. Occasionally, a "leap second" is added to UTC to keep it in sync with UT (which changes because of variations in Earth's rotation rate).

Table 2-1. Values of ΔT Derived from Historical Records

Year	ΔT (seconds)	Standard Error (seconds)
–500	17,190	430
–400	15,530	390
–300	14,080	360
–200	12,790	330
–100	11,640	290
0	10,580	260
100	9,600	240
200	8,640	210
300	7,680	180
400	6,700	160
500	5,710	140
600	4,740	120
700	3,810	100
800	2,960	80
900	2,200	70
1000	1,570	55
1100	1,090	40
1200	740	30
1300	490	20
1400	320	20
1500	200	20
1600	120	20
1700	9	5
1750	13	2
1800	14	1
1850	7	< 1
1900	–3	< 1
1950	29	< 0.1

In modern times, the determination of ΔT is made using atomic clocks and radio observations of quasars, so it is completely independent of the lunar ephemeris. Table 2-2 gives the value of ΔT every five years from 1955 to 2005 (*Astronomical Almanac for 2006*, page K9).

Table 2-2. Recent Values of ΔT from Direct Observations

Year	ΔT (seconds)	5-Year Change (seconds)	Average 1-Year Change (seconds)
1955.0	+31.1	—	—
1960.0	+33.2	2.1	0.42
1965.0	+35.7	2.5	0.50
1970.0	+40.2	4.5	0.90
1975.0	+45.5	5.3	1.06
1980.0	+50.5	5.0	1.00
1985.0	+54.3	3.8	0.76
1990.0	+56.9	2.6	0.52
1995.0	+60.8	3.9	0.78
2000.0	+63.8	3.0	0.60
2005.0	+64.7	0.9	0.18

The average annual change of ΔT was 0.99 s from 1965 to 1980, however, the average annual increase was just 0.63 s from 1985 to 2000, and only 0.18 s from 2000 to 2005. Future changes and trends in ΔT can not be predicted with certainty because theoretical models of the physical causes are not of high enough precision. Extrapolations from the table weighted by the long period trend from tidal braking of the Moon offer reasonable estimates of +67 s in 2010, +93 s in 2050, +203 s in 2100, and +442 s in 2200.

Outside the period of observations (500 BCE to 2005 CE), the value of ΔT can be extrapolated from measured values using the long-term mean parabolic trend:

$$\Delta T = -20 + 32\,u^2 \text{ s}, \tag{9}$$

where u = (year – 1820)/100, and is defined as time measured in centuries.

2.7 Polynomial Expressions for ΔT

Using the ΔT values derived from the historical record and from direct observations (Tables 2-1 and 2-2, respectively), a series of polynomial expressions have been created to simplify the evaluation of ΔT for any time during the interval –1999 to +3000. We define the decimal year "*y*" as follows:

$$y = \text{year} + (\text{month} - 0.5)/12. \tag{10}$$

This gives y for the middle of the month, which is accurate enough given the precision in the known values of ΔT. The following polynomial expressions can be used to calculate the value of ΔT (in seconds) over the interval of the *Canon*.

Before the year –500, calculate

$$\Delta T = -20 + 32\,u^2, \tag{11}$$

where u = (y – 1820)/100.

Between years –500 and +500, we use the data from Table 2-1, except that for the year –500 we changed the value 17,190 to 17,203.7 in order to avoid a discontinuity with the previous formula (11) at that epoch. The value for ΔT is given by a polynomial of the 6th degree, which reproduces the values in Table 2-1 with an error not larger than 4 s:

$$\Delta T = 10583.6 - 1014.41\,u + 33.78311\,u^2 - 5.952053\,u^3$$

$$-0.1798452\,u^4 + 0.022174192\,u^5 + 0.0090316521\,u^6 \tag{12}$$

where $u = y/100$.

Between years 500 and 1600, we again use the data from Table 2-1. Calculate $u = (y - 1000)/100$. The value for ΔT is given by the following polynomial of the 6th degree with a divergence from Table 2-1 not larger than 4 s:

$$\Delta T = 1574.2 - 556.01\,u + 71.23472\,u^2 + 0.319781\,u^3$$

$$- 0.8503463\,u^4 - 0.005050998\,u^5 + 0.0083572073\,u^6, \tag{13}$$

where $u = (y - 1000)/100$.

Between years 1600 and 1700, calculate

$$\Delta T = 120 - 0.9808\,t - 0.01532\,t^2 + (t^3 / 7129), \tag{14}$$

where $t = y - 1600$, and is defined as time measured in years.

Between years 1700 and 1800, calculate

$$\Delta T = 8.83 + 0.1603\,t - 0.0059285\,t^2 + 0.00013336\,t^3 - (t^4 / 1{,}174{,}000), \tag{15}$$

where $t = y - 1700$.

Between years +1800 and +1860, calculate

$$\Delta T = 13.72 - 0.332447\,t + 0.0068612\,t^2 + 0.0041116\,t^3 - 0.00037436\,t^4$$

$$+ 0.0000121272\,t^5 - 0.0000001699\,t^6 + 0.000000000875\,t^7, \tag{16}$$

where $t = y - 1800$.

Between years 1860 and 1900, calculate

$$\Delta T = 7.62 + 0.5737\,t - 0.251754\,t^2 + 0.01680668\,t^3 - 0.0004473624\,t^4 + (t^5 / 233{,}174), \tag{17}$$

where $t = y - 1860$.

Between years 1900 and 1920, calculate

$$\Delta T = -2.79 + 1.494119\,t - 0.0598939\,t^2 + 0.0061966\,t^3 - 0.000197\,t^4, \tag{18}$$

where $t = y - 1900$.

Between years 1920 and 1941, calculate

$$\Delta T = 21.20 + 0.84493\,t - 0.076100\,t^2 + 0.0020936\,t^3, \tag{19}$$

where $t = y - 1920$.

Between years 1941 and 1961, calculate

$$\Delta T = 29.07 + 0.407\,t - (t^2/233) + (t^3 / 2547), \tag{20}$$

where $t = y - 1950$.

Between years 1961 and 1986, calculate

$$\Delta T = 45.45 + 1.067\,t - (t^2/260) - (t^3 / 718), \tag{21}$$

where $t = y - 1975$.

Between years 1986 and 2005, calculate

$$\Delta T = 63.86 + 0.3345\,t - 0.060374\,t^2 + 0.0017275\,t^3 + 0.000651814\,t^4 + 0.00002373599\,t^5, \tag{22}$$

where $t = y - 2000$.

Between years 2005 and 2050, calculate

$$\Delta T = 62.92 + 0.32217\,t + 0.005589\,t^2, \tag{23}$$

where $t = y - 2000$.

This expression is derived from estimated values of ΔT in the years 2010 and 2050. The value for 2010 (66.9 s) is based on a linear extrapolation from 2005 using 0.39 s/y (average from 1995 to 2005). The value for 2050 (93 s) is linearly extrapolated from 2010 using 0.66 s/y (average rate from 1901 to 2000).

Between years 2050 and 2150, calculate

$$\Delta T = -20 + 32\,[(y - 1820)/100]^2 - 0.5628\,(2150 - y). \tag{24}$$

The last term is introduced to eliminate the discontinuity at 2050.

After 2150, calculate

$$\Delta T = -20 + 32\,u^2, \tag{25}$$

where $u = (y - 1820)/100$.

All values of ΔT based on Morrison and Stephenson (2004) assume a value for the Moon's secular acceleration of –26 arcsec/cy^2. However, the ELP-2000/82 lunar ephemeris employed in the *Canon* uses a slightly different value of –25.858 arcsec/cy^2. Thus, a small correction "*c*" must be added to the values derived from the polynomial expressions for ΔT before they can be used in the *Canon*:

$$c = -0.000012932\,(y - 1955)^2. \tag{26}$$

Because the values of ΔT for the interval 1955 to 2005 were derived independent of any lunar ephemeris, no correction is needed for this period.

2.8 Uncertainty in ΔT

The uncertainty in the value of ΔT is of particular interest in the calculation of eclipse paths in the distant past and future. Unfortunately, estimating the standard error in ΔT prior to 1600 CE is a difficult problem. It depends on a number of factors which include the accuracy of determining ΔT from historical eclipse records and modeling the physical processes producing changes in Earth's rotation. Morrison and Stephenson (2004) propose a simple parabolic relation to estimate the standard error (σ), which is valid over the period 1000 BCE to 1200 CE:

$$\sigma = 0.8\,t^2 \text{ s,} \tag{27}$$

where t = (year – 1820)/100.

Table 2-3 gives the errors in ΔT along with the corresponding uncertainties in the longitude of an eclipse path.

Table 2-3. Uncertainty of ΔT, Part I

Year	σ (seconds)	Longitude
–1000	636	2.65°
–500	431	1.79°
0	265	1.10°
+500	139	0.58°
+1000	54	0.22°
+1200	31	0.13°

The decade fluctuations in ΔT result in an uncertainty of approximately 20 s (0.08°) for the period 1300 to 1600 CE.

During the telescopic era (1600 CE to present), records of astronomical observations pin down the decade fluctuations with increasing reliability. The uncertainties in ΔT are presented in Table 2-4 (Stephenson and Houlden, 1986).

Table 2-4. Uncertainty of ΔT, Part II

Year	σ (seconds)	Longitude
+1700	5	0.021°
+1800	1	0.004°
+1900	0.1	0.0004°

The estimation in the uncertainty of ΔT prior to 1000 BCE must rely on a certain amount of modeling and theoretical arguments because no measurements of ΔT are available for this period. Huber (2000) proposed a Brownian motion model including drift to estimate the standard error in ΔT for periods outside the epoch of measured values. The intrinsic variability in the LOD during the 2,500 years of observations (500 BCE to 2000 CE) is 1.780 ms/cy with a standard error of 0.56 ms/cy. This rate is not due entirely to tidal friction, but includes a drift in LOD from imperfectly understood effects, such as changes in sea level due to variations in polar ice caps. Presumably, the same mechanisms operating during the present era also operated prior to 1000 BCE, as well as one millennium into the future.

Huber's derived estimate for the total standard error (fluctuations plus drift) in ΔT is as follows.

$$\sigma = 365.25\ \text{N SQRT}\,[(\text{N Q} / 3)\ (\,1 + \text{N} / \text{M})]\ /\ 1000, \tag{28}$$

where:

N = Difference between target year and calibration year;
M = 2500 years (–500 to +2000)—this covers the period of observed ΔT measurements; and
Q = 0.058 ms^2/yr.

The calibration year is taken as –500 for target years before 500 BCE, while the calibration year is 2005 CE for target years in the future. Evaluation of this expression at 500-year intervals is found in Table 2-5. It shows estimates in the standard error of ΔT along with the equivalent shift in longitude

Table 2-5. Uncertainty of ΔT, Part III

Year	σ (seconds)	Longitude
–4500	20,717	86.3°
–4000	16,291	67.9°
–3500	12,378	51.6°
–3000	8,978	37.4°
–2500	6,094	25.4°
–2000	3,732	15.6°
–1500	1,900	7.9°
–1000	622	2.6°
—	—	—
+2500	612	2.6°
+3000	1,885	7.9°
+3500	3,711	15.6°
+4000	6,068	25.3°
+4500	8,946	37.3°
+5000	12,341	51.4°

Section 3: Eclipse Statistics

3.1 Statistical Distribution of Eclipse Types

Eclipses of the Sun can only occur during the New Moon phase. It is then possible for the Moon's penumbral, umbral, or antumbral shadows to sweep across Earth's surface thereby producing an eclipse. There are four types of solar eclipses:

1) Partial—Moon's penumbral shadow traverses Earth (umbral and antumbral shadows completely miss Earth)
2) Annular—Moon's antumbral shadow traverses Earth (Moon is too far from Earth to completely cover the Sun)
3) Total—Moon's umbral shadow traverses Earth (Moon is close enough to Earth to completely cover the Sun)
4) Hybrid—Moon's umbral and antumbral shadows traverse Earth (eclipse appears annular and total along different sections of its path). Hybrid eclipses are also known as annular-total eclipses.

During the 5000-year period from –1999 to +3000 (2000 BCE to 3000 CE), Earth will experience 11,898 eclipses of the Sun. The statistical distribution of the four basic eclipse types over this interval is shown in Table 3-1.

Table 3-1. Distribution of Basic Eclipse Types

Eclipse Type	Abbreviation	Number	Percent
All Eclipses	—	11,898	100.0%
Partial	P	4,200	35.3%
Annular	A	3,956	33.2%
Total	T	3,173	26.7%
Hybrid	H	569	4.8%

All partial eclipses are events in which some portion of the Moon's penumbral shadow passes across Earth's surface. In comparison all annular, total, and hybrid eclipses can be characterized as events in which some portion of the Moon's umbral and/or antumbral shadow crosses Earth.

In the case of umbral or antumbral eclipses (annular, total, or hybrid), they can be further categorized as:

a) Central (two limits)—The central axis of the Moon's umbral or antumbral shadow traverses Earth, thereby producing a central line in the eclipse track. The umbra or antumbra falls entirely upon Earth producing a ground track with both a northern and southern limit.
b) Central (one limit)—The central axis of the Moon's umbral or antumbral shadow traverses Earth, however, a portion of the umbra or antumbra misses Earth throughout the eclipse, thereby producing a ground track with just one limit.
c) Non-Central—The central axis of the Moon's umbral or antumbral shadow misses Earth, however, one edge of the umbra or antumbra grazes Earth, thereby producing a ground track with one limit and no central line.

Using the above categories, the distribution of the 3,956 annular eclipses is shown in Table 3-2.

Table 3-2. Statistics of Annular Eclipses

Annular Eclipses	Number	Percent
All Annular Eclipses	3,956	100.0%
Central (two limits)	3,827	96.7%
Central (one limit)	61	1.5%
Non-Central (one limit)	68	1.7%

Examples of central annular eclipses with one limit include: 1874 Oct 10, 2003 May 31, 2044 Feb 28, and 2101 Feb 28. Some examples of non-central annular eclipses are: 1950 Mar 18, 1957 Apr 30, 2014 Apr 29, and 2043 Oct 03.

Similarly, the distribution of the 3,173 total eclipses is shown in Table 3-3.

Table 3-3. Statistics of Total Eclipses

Total Eclipses	Number	Percent
All Total Eclipses	3,173	100.0%
Central (two limits)	3,121	98.4%
Central (one limit)	26	0.8%
Non-Central (one limit)	26	0.8%

Examples of central total eclipses with one limit include: 1494 Mar 07, 1523 Aug 11, 2185 Jul 26, and 2195 Aug 05. The most recent examples of non-central total eclipses are: 1957 Oct 23, 1967 Nov 02, 2043 Apr 09, and 2459 Jun 01.

All 569 hybrid eclipses are central with two limits. Hybrid eclipses with a single limit (both central and non-central) are exceedingly rare. An estimate of the mean frequency of non-central hybrid eclipses is one out of every 600 million eclipses or once every 250 million years (Meeus, 2002).

The central path of most hybrid eclipses begins annular, changes to total, and finally reverts back to annular. This combination (ATA) occurs in 519 out of the 569 hybrid eclipses in the *Canon*. However, there are two other possibilities. If the vertex of the Moon's umbral shadow passes through Earth's fundamental plane during the eclipse, then the hybrid eclipse can begin as total and end as annular (TA) or it can begin as annular and end as total (AT). Table 3-4 shows the distribution of the three different classes of hybrid eclipses.

Table 3-4. Statistics of Hybrid Eclipses

Hybrid Eclipses	Number	Percent
All Hybrid Eclipses	569	100.0%
Hybrid (ATA)	519	91.2%
Hybrid (TA)	24	4.2%
Hybrid (AT)	26	4.6%

Examples of ATA hybrid eclipses include: 1986 Oct 03, 1987 Mar 29, 2005 Apr 08, and 2023 Apr 20. Examples of the relatively rare TA hybrid eclipse are: 1564 Jun 08, 1703 Jan 17, 1825 Dec 09, and 2386 Apr 29. Finally, some examples of the rare AT hybrid eclipse include: 1489 Jun 28, 1854 Nov 20, 2013 Nov 03, and 2172 Oct 17.

3.2 Distribution of Eclipse Types by Century

Table 3-5 summarizes 5,000 years of eclipses by eclipse type in 100-year intervals. The number of central and non-central (in square brackets) events are given for annular and total eclipses. The number of eclipses in any one century ranges from 222 to 255 with an average of 238.0. Over the 1,000-year interval of 1501 to 2500 CE (centered on the present era), the average is 238.9 eclipses per century.

Some remarkable patterns are present in this table. There exists a cyclical variation in the number of eclipses per century with a length of a little under six centuries, giving alternating "rich" and "poor" periods (Meeus, 1997). The 20th and 21st centuries (1901–2100) are poor periods, with only 228 and 224 eclipses, respectively. This cycle is also present when only central eclipses are considered.

The cycle appears to have a period of approximately 600 years with an amplitude of ~30 eclipses. This is close to a known eclipse period called the "tetradia," which has a period of 586.02 years. The tetradia governs the recurrence of tetrads or groups of four successive total lunar eclipses each separated by six lunations. The tetradia cycle for lunar eclipse tetrads appears to be 180 degrees out of phase with the cycle for solar eclipses. When there are many tetrads, there are fewer solar eclipses. We are currently in a tetrad-rich period with tetrads in 2003 to 2004, 2014 to 2015, and 2032 to 2033.

The number of hybrid solar eclipses per century also varies cyclically with a period of approximately 17 centuries.

Table 3-5. Eclipse Types by Century: –1999 to +3000 (2000 BCE to 3000 CE)

Century Interval	Number of Eclipses	Number of Partial Eclipses	Number of Annular Eclipses*	Number of Total Eclipses*	Number of Hybrid Eclipses
–1999 to –1900	239	84	70 [1]	62 [0]	22
–1899 to –1800	253	93	80 [0]	62 [1]	17
–1799 to –1700	254	95	73 [1]	63 [1]	21
–1699 to –1600	230	75	70 [1]	60 [0]	24
–1599 to –1500	225	78	65 [2]	59 [0]	21
–1499 to –1400	226	77	65 [4]	61 [1]	18
–1399 to –1300	234	76	83 [1]	68 [0]	6
–1299 to –1200	250	93	86 [0]	64 [0]	7
–1199 to –1100	252	93	89 [0]	63 [0]	7
–1099 to –1000	238	79	89 [2]	67 [1]	0
–0999 to –0900	226	84	74 [1]	58 [3]	6
–0899 to –0800	225	80	73 [2]	64 [2]	4
–0799 to –0700	234	79	88 [0]	64 [0]	3
–0699 to –0600	253	96	86 [1]	63 [0]	7
–0599 to –0500	255	96	85 [1]	65 [0]	8
–0499 to –0400	241	84	76 [2]	62 [0]	17
–0399 to –0300	225	83	62 [1]	56 [0]	23
–0299 to –0200	226	83	61 [1]	55 [2]	24
–0199 to –0100	237	80	71 [2]	62 [1]	21
–0099 to 0000	251	92	77 [0]	64 [1]	17

Table 3-5. (Cont.) Eclipse Types by Century: –1999 to +3000 (2000 BCE to 3000 CE)

Century Interval	Number of Eclipses	Number of Partial Eclipses	Number of Annular Eclipses*	Number of Total Eclipses*	Number of Hybrid Eclipses
0001 to 0100	248	90	74 [1]	58 [0]	25
0101 to 0200	237	80	75 [2]	63 [1]	16
0201 to 0300	227	79	70 [4]	69 [0]	5
0301 to 0400	222	73	74 [2]	65 [1]	7
0401 to 0500	233	80	83 [1]	67 [0]	2
0501 to 0600	251	93	86 [1]	65 [0]	6
0601 to 0700	251	90	89 [1]	67 [0]	4
0701 to 0800	233	77	86 [2]	66 [0]	2
0801 to 0900	222	78	72 [2]	62 [2]	6
0901 to 1000	227	76	83 [1]	65 [1]	1
1001 to 1100	241	84	90 [0]	61 [0]	6
1101 to 1200	250	92	82 [0]	61 [0]	15
1201 to 1300	246	87	80 [1]	60 [0]	18
1301 to 1400	229	76	72 [3]	54 [0]	24
1401 to 1500	222	77	62 [3]	60 [1]	19
1501 to 1600	228	75	69 [3]	62 [0]	19
1601 to 1700	248	89	74 [0]	60 [1]	24
1701 to 1800	251	92	78 [0]	62 [0]	19
1801 to 1900	242	87	77 [0]	63 [0]	15
1901 to 2000	228	78	71 [2]	68 [3]	6
2001 to 2100	224	77	70 [2]	67 [1]	7
2101 to 2200	235	79	82 [5]	65 [0]	4
2201 to 2300	248	92	86 [0]	67 [0]	3
2301 to 2400	248	88	86 [0]	66 [0]	8
2401 to 2500	237	81	87 [2]	65 [1]	1
2501 to 2600	225	83	71 [1]	63 [1]	6
2601 to 2700	227	77	78 [3]	64 [0]	5
2701 to 2800	242	84	92 [0]	63 [0]	3
2801 to 2900	254	95	86 [1]	63 [0]	9
2901 to 3000	248	91	80 [2]	64 [0]	11

* The first quantity is the number of central eclipses, while the second quantity, in square brackets [ ], is the number of non-central eclipses.

3.3 Distribution of Eclipse Types by Month

Table 3-6 summarizes 5,000 years of eclipses by eclipse type in each month of the year. The first value in each column is the number of eclipses of a given type for the corresponding month. The second number in square brackets [ ] is the number of eclipses divided by the number of days in that month. This normalization allows direct comparison of eclipse frequencies in different months.

A brief examination of the values in the column "Number of All Eclipses" shows that eclipses are equally distributed around the year. The same holds true for partial eclipses; however, the columns for annular and total eclipses reveal something interesting. Annular eclipses are 1 1/3 times more likely during the period of November–December–January compared to the months May–June–July. This effect is attributed to Earth's elliptical orbit. Earth currently reaches perihelion in early January and aphelion in early July. Consequently, the Sun's apparent diameter varies from 1,952 to 1,887 arcsec between perihelion and aphelion. The Sun's larger apparent diameter at perihelion makes annular eclipses more frequent at that time.

The opposite argument holds true for total eclipses which are nearly 1 1/2 times more likely during the period May–June–July compared to the months November–December–January. In this case, the Sun's smaller apparent size around aphelion increases the frequency of total eclipses at that time. Total eclipses actually outnumber annular eclipses during the season May–June–July (Meeus, 2002).

Table 3-6. Eclipse Types by Month: –1999 to +3000 (2000 BCE to 3000 CE)

Month	Number of All Eclipses	Number of Partial Eclipses	Number of Annular Eclipses	Number of Total Eclipses	Number of Hybrid Eclipses
January	1010 [32.6]	357 [11.5]	380 [12.3]	222 [7.2]	51 [1.6]
February	919 [32.8]	317 [11.3]	334 [11.9]	225 [8.0]	43 [1.5]
March	1009 [32.5]	359 [11.6]	319 [10.3]	280 [9.0]	51 [1.6]
April	981 [32.7]	345 [11.5]	294 [9.8]	299 [10.0]	43 [1.4]
May	1009 [32.5]	353 [11.4]	294 [9.5]	313 [10.1]	49 [1.6]
June	973 [32.4]	348 [11.6]	279 [9.3]	310 [10.3]	36 [1.2]
July	1008 [32.5]	354 [11.4]	299 [9.6]	312 [10.1]	43 [1.4]
August	1008 [32.5]	358 [11.5]	308 [9.9]	303 [9.8]	39 [1.3]
September	982 [32.7]	354 [11.8]	333 [11.1]	248 [8.3]	47 [1.6]
October	1008 [32.5]	355 [11.5]	362 [11.7]	230 [7.4]	61 [2.0]
November	977 [32.6]	344 [11.5]	367 [12.2]	210 [7.0]	56 [1.9]
December	1014 [32.7]	356 [11.5]	387 [12.5]	221 [7.1]	50 [1.6]

(Numbers in square brackets [ ] are number of eclipses divided by the number of days in the month.)

3.4 Eclipse Frequency and the Calendar Year

There are 2 to 5 solar eclipses in every calendar year. Table 3-7 shows the distribution in the number of eclipses per year for the 5,000 years covered in the *Canon*.

Table 3-7. Number of Eclipses per Year

Number of Eclipses per Year	Number of Years	Percent
2	3,625	72.5%
3	877	17.5%
4	473	9.5%
5	25	0.5%

When two eclipses occur in one calendar year, they can be any combination of P, A, T, or H (partial, annular, total, or hybrid, respectively) with the one exception that they can not both be T. Table 3-8 lists the frequency of each eclipse combination along with five recent years when the combination occurs. The table makes no distinction in the order of any two eclipses. For example, the eclipse combination PA includes all years where the order is either PA or AP.

Table 3-8. Two Eclipses in One Year

Eclipse Combinations[a]	Number of Years	Percent	Examples (Years) [b]
PP	177	4.9%	…, 2004, 2007, 2022, 2025, 2040, …
PA	97	2.7%	…, 2014, 2032, 2101, 2102, 2119, …
PH	19	0.5%	…, 0227, 0245, 1909, 1986, 2050]
PT	236	6.5%	…, 2015, 2033, 2037, 2055, 2068, …
AA	292	8.1%	…, 1951, 1969, 2056, 2074, 2085, …
AH	239	6.6%	…, 2005, 2013, 2023, 2031, 2049, …
AT	2402	66.3%	…, 2006, 2008, 2009, 2010, 2012, …
HH	84	2.3%	…, 1753, 1771, 1789, 1807, 1825]
HT	79	2.2%	…, 1843, 1894, 1912, 1930, 2910, …

a. P = Partial, A = Annular, T = Total, and H = Hybrid.
b. When years end with a square bracket], there are no other examples beyond the last year.

When three eclipses occur in one calendar year, there are 14 possible combinations of P, A, T, or H. Table 3-9 lists the frequency of each eclipse combination along with five recent years when each combination occurs. The table makes no distinction in the order of eclipses in any combination. For example, the eclipse combination PAT includes all years where the order is PAT, PTA, APT, ATP, TAP, and TPA. The rarest combinations—PHT and AAH (actually HTP and AHA, respectively)—each occurred only twice in the five millennium span of this work.

Table 3-9. Three Eclipses in One Year

Eclipse Combinations[a]	Number of Years	Percent	Examples (Years) [b]
PPP	396	45.2%	…, 1971, 2018, 2036, 2054, 2058, …
PPA	71	8.1%	…, 1722, 1740, 1899, 2224, 2242, …
PPH	7	0.8%	[–1906, –1888, –1794, –0224, 1544, 1609, 1703]
PPT	74	8.4%	…, 1834, 1852, 1928, 2130, 2271, …
PAA	18	2.1%	…, 0650, 0791, 1704, 2419, 2437, …
PAH	5	0.6%	[–1907, –0457, –0316, –0101, –0055]
PAT	145	16.5%	…, 1992, 2019, 2084, 2149, 2225, …
PHH	5	0.6%	[–1683, –0037, –0019, –0001, 1768]
PHT	2	0.2%	[–1488, 1786]
AAH	2	0.2%	[–1944, 1489]
AAT	102	11.6%	…, 1954, 1973, 2038, 2103, 2122, …
AHH	8	0.9%	[–484, –0400, –0139, 1144, 1228, 1339, 1405, 1666]
AHT	13	1.5%	[–1833, –1702, –1507, –0660, –0465, –0419, –0074, 0121, 1163, 1386, 1731, 1908, 2950]
ATT	29	3.3%	…, 1554, 1712, 1889, 2057, 2252, …

a. P = Partial, A = Annular, T = Total, and H = Hybrid.

b. When years are enclosed in square brackets [ ], they include all examples in 5,000 years.

When four eclipses occur in one calendar year, there are seven possible combinations of eclipse types P, A, T, and H. Table 3-10 lists the frequency of each eclipse combination along with five recent years when each combination occurs. The table makes no distinction in the order of eclipses in the seven combinations. The rarest combination—PPAH (actually HAPP)—occurred only once in year –1748 (1749 BCE).

Table 3-10. Four Eclipses in One Year

Eclipse Combinations[a]	Number of Years	Percent	Examples (Years) [b]
PPPP	327	69.1%	…, 2000, 2011, 2029, 2047, 2065, …
PPPA	79	16.7%	…, 1758, 1917, 2141, 2159, 2177, …
PPPH	7	1.5%	[–1925, –1870, –0120, 1573, 1591, 1685, 1750]
PPPT	41	8.7%	…, 1693, 1870, 2076, 2094, 2112, …
PPAA	3	0.6%	[–1209, –1032, 0596]
PPAH	1	0.2%	[–1748]
PPAT	15	3.2%	[–1795, –1162, –0688, –0641, –0576, –0511, –0446, 0010, 0075, 0661, 1182, 1880, 2195, 2782, 2912]

a. P = Partial, A = Annular, T = Total, and H = Hybrid.

b. When years are enclosed in square brackets [ ], they include all examples in 5,000 years.

The maximum number of five solar eclipses in one calendar year is quite rare. Over the 5,000-year span of the *Canon,* there are only 25 years containing five solar eclipses. They occur in three possible combinations of eclipse types where four out of the five eclipses are always of type P. The first eclipse of such a quintet always occurs in the first half of January, while the last eclipse falls in the latter half of December. Table 3-11 lists all 25 years containing five eclipses along with their eclipse combinations and frequencies. The rarest combination—PPPPH—occurred only once in year –1852 (1853 BCE). Once again, the table makes no distinction in the order of eclipses in any combination.

Table 3-11. Five Eclipses in One Year

Eclipse Combinations[a]	Number of Years	Percent	All Examples (Years)
PPPPA	18	72.0%	–1805, –1787, –1675, –1089, –0568, –0503, –0373, 0018, 0148, 0604, 0734, 1255, 1805, 1935, 2206, 2709, 2839, 2904
PPPPH	1	4.0%	–1852
PPPPT	6	24.0%	–1740, –1154, –0438, 0083, 0669, 2774

a. P = Partial, A = Annular, T = Total, and H = Hybrid.

3.5 Extremes in Eclipse Magnitude—Partial Eclipses

Eclipse magnitude is defined as the fraction of the Sun's diameter covered by the Moon. It reaches a maximum value at the instant of greatest eclipse. A search through the 11,898 eclipses in the *Canon* reveals some interesting cases involving extreme values of the eclipse magnitude.

Thirteen partial eclipses have a maximum magnitude less than 0.005 (Table 3-12). These events are all the first or last members in a Saros series. The smallest magnitude was the partial eclipse of –1838 Apr 04 with a magnitude of just 0.00002.

Table 3-12. Partial Eclipses with Magnitude 0.005 or Less

Date (Dynamical Time)	Saros	Gamma	Eclipse Magnitude
–1838 Apr 04	–10	1.5615	0.00002
–1512 Apr 29	43	1.5386	0.0041
–0756 Mar 12	66	–1.5417	0.0047
0662 Jun 21	115	1.5377	0.0030
0929 Jul 09	80	1.5267	0.0049
1175 Oct 16	91	–1.5690	0.0019
1512 Apr 16	140	–1.5289	0.0003
1639 Jan 04	145	1.5650	0.0009
1935 Jan 05	111	–1.5381	0.0013
2883 Aug 23	188	–1.5524	0.0010
2893 Dec 29	146	1.5706	0.0028
2904 Jun 05	142	1.5428	0.0040
2995 Aug 17	190	–1.5542	0.0036

Table 3-13 lists the eight partial eclipses having a maximum magnitude greater than 0.995. The greatest partial eclipse occurred on –1577 Mar 30 with a maximum magnitude of 0.9998.

Table 3-13. Partial Eclipses with Magnitude 0.995 or More

Date (Dynamical Time)	Saros	Gamma	Eclipse Magnitude
–1585 Mar 28	33	1.0137	0.9960
–1577 Mar 30	4	1.0109	0.9998
–0944 Sep 14	29	–1.0056	0.9987
–0927 Nov 04	57	1.0005	0.9990
–0018 Jun 10	56	1.0154	0.9954
0257 Aug 26	68	1.0060	0.9969
0654 May 22	106	–1.0131	0.9990
1750 Jul 03	142	–0.9985	0.9956

3.6 Extremes in Eclipse Magnitude—Annular Eclipses

Sixteen annular eclipses have a maximum magnitude (at greatest eclipse) less than or equal to 0.910 (Table 3-14). Ten of these events are central with two limits, four are central with one limit, and two are non-central (with one limit). The annular eclipses with the smallest magnitude (at greatest eclipse) occurred on –1682 Nov 12 and 1601 Dec 24 and had a magnitude of just 0.9078.

Table 3-14. Annular Eclipses with Magnitude 0.910 or Less

Date (Dynamical Time)	Saros	Gamma	Eclipse Magnitude	Central Duration
–1718 Oct 21	6	0.9195	0.9091	08m 18s
–1700 Oct 31	6	0.9254	0.9081	08m 44s
–1682 Nov 12	6	0.9295	0.9078	09m 08s
–1664 Nov 22	6	0.9323	0.9083	09m 26s
–1646 Dec 03	6	0.9353	0.9095	09m 36s
–0984 Nov 04 [a]	27	–1.0234	0.9099	–
0123 Nov 06 [b]	64	0.9783	0.9098	08m 20s
0141 Nov 16 [b]	64	0.9854	0.9089	08m 31s
0159 Nov 27 [b]	64	0.9908	0.9087	08m 34s
0177 Dec 08 [b]	64	0.9944	0.9093	08m 28s
1565 Nov 22	135	0.9564	0.9092	09m 37s
1583 Dec 14	135	0.9471	0.9083	10m 03s
1601 Dec 24	135	0.9402	0.9078	10m 14s
1620 Jan 04	135	0.9321	0.9081	10m 13s
1638 Jan 15	135	0.9242	0.9090	10m 00s
2485 Dec 07 [a]	140	1.0242	0.9100	–

a. Non-central annular eclipse (with one limit).
b. Central annular eclipse with one limit.

Seventeen annular eclipses have a maximum magnitude (at greatest eclipse) greater than or equal to 0.9995 (Table 3-15). All of these events have central durations (i.e., central line duration at greatest eclipse) lasting 3 s or less. The annular eclipse with the largest magnitude (at greatest eclipse) occurs on 2931 Dec 30 with a magnitude of 0.99998.

Table 3-15. Annular Eclipses with Magnitude 0.9995 or More

Date (Dynamical Time)	Saros	Gamma	Eclipse Magnitude	Central Duration
–1800 Apr 03	10	0.1778	0.9997	00m 02s
–1734 Sep 18	26	–0.5105	0.9995	00m 03s
–1725 Mar 17	2	0.8105	0.9997	00m 01s
–1624 Oct 02	8	0.9377	0.9995	00m 02s
–1590 Jun 20	21	–0.0376	0.9997	00m 02s
–1482 Feb 27	16	0.3992	0.9997	00m 02s
–1326 Apr 14	27	0.0409	0.9996	00m 02s
–0124 Sep 07	81	0.7642	0.9999	00m 00s
1087 Aug 01	111	0.1644	0.9996	00m 02s
1384 Aug 17	125	0.5354	0.9999	00m 01s
1704 Nov 27	118	0.6716	0.9999	00m 01s
1822 Feb 21	137	0.6914	0.9996	00m 02s
1858 Mar 15	137	0.6461	0.9996	00m 02s
1876 Mar 25	137	0.6142	0.9999	00m 01s
1948 May 09	137	0.4133	0.9999	00m 00s
2862 Sep 15	158	0.5956	0.9999	00m 01s
2931 Dec 30	166	0.1511	0.99998	00m 00s

3.7 Extremes in Eclipse Magnitude—Total Eclipses

Nineteen total eclipses have a maximum magnitude less than or equal to 1.0075 (Table 3-16). Six of these eclipses are central while the remaining 13 are non-central. The smallest magnitude was the total eclipse of –0839 Jul 26 with a magnitude of just 1.0002.

Table 3-16. Total Eclipses with Magnitude 1.0075 or Less

Date (Dynamical Time)	Saros	Gamma	Eclipse Magnitude	Central Duration
–1038 Apr 09 [a]	22	1.0023	1.0034	–
–0915 Feb 28 [b]	25	–1.0012	1.0004	–
–0909 Nov 15 [a]	57	0.9976	1.0050	–
–0905 Mar 10 [b]	54	–1.0053	1.0072	–
–0839 Jul 26 [a]	32	1.0095	1.0002	–
–0829 Aug 05 [a]	61	0.9972	1.0064	–
–0159 Jul 08 [b]	53	–1.0096	1.0051	–
0854 Feb 01	83	–0.9582	1.0065	00m 22s
0861 Sep 08 [b]	87	–1.0032	1.0053	–
0865 Jan 01	84	0.9518	1.0073	00m 36s
0883 Jan 12	84	0.9609	1.0057	00m 27s
0890 Feb 23 [b]	83	–1.0005	1.0005	–
0901 Jan 23	84	0.9731	1.0042	00m 19s
0919 Feb 03	84	0.9909	1.0020	00m 09s
0994 Aug 09 [a]	119	0.9985	1.0017	–
1957 Oct 23 [b]	123	–1.0022	1.0013	–
2459 Jun 01 [b]	164	–1.0097	1.0038	–
2518 Mar 12	138	0.9200	1.0071	00m 31s
2542 Dec 08 [b]	170	–0.9975	1.0072	–

a. Non-central total eclipse at high northern latitudes.
b. Non-central total eclipse at high southern latitudes.

Sixteen total eclipses have a maximum magnitude greater than or equal to 1.080. Their central durations all exceed 6 min with nearly half exceeding 7 min. Note that these eclipses all take place during the period of the year when Earth is near the aphelion of its orbit (May to July), resulting in a smaller than normal diameter of the solar disk. The total eclipse with the largest magnitude (1.0813) occurred on 0504 May 29. The total eclipse with the longest duration of totality occurs on 2186 Jul 16 with a magnitude of 1.0805. The 16 eclipses in Table 3-17 belong to just five Saros series.

Table 3-17. Total Eclipses with Magnitude 1.080 or More

Date (Dynamical Time)	Saros	Gamma	Eclipse Magnitude	Central Duration
–1337 May 14	26	0.1487	1.0801	06m 51s
–1319 May 25	26	0.2236	1.0807	06m 41s
–1301 Jun 05	26	0.2982	1.0805	06m 25s
–1160 May 07	29	–0.2990	1.0806	06m 45s
–1142 May 18	29	–0.3742	1.0809	06m 56s
–1124 May 28	29	–0.4490	1.0804	07m 03s
0327 Jun 06	81	–0.0413	1.0810	07m 03s
0345 Jun 16	81	–0.1162	1.0811	07m 17s
0363 Jun 27	81	–0.1899	1.0804	07m 24s
0486 May 19	84	0.1193	1.0806	06m 54s
0504 May 29	84	0.1927	1.0813	06m 44s
0522 Jun 10	84	0.2675	1.0812	06m 28s
0540 Jun 20	84	0.3414	1.0801	06m 07s
2150 Jun 25	139	–0.0910	1.0802	07m 14s
2168 Jul 05	139	–0.1660	1.0807	07m 26s
2186 Jul 16	139	–0.2396	1.0805	07m 29s

3.8 Extremes in Eclipse Magnitude—Hybrid Eclipses

Fourteen hybrid eclipses have a maximum magnitude (at greatest eclipse) less than or equal to 1.00025. All of these events are central with a central duration of totality of 1 s or less.

Table 3-18. Hybrid Eclipses with Magnitude 1.00025 or Less

Date (Dynamical Time)	Saros	Gamma	Eclipse Magnitude	Central Duration
–1747 Nov 10	5	–0.7406	1.0001	00m 00s
–1716 Sep 28	26	–0.4927	1.0002	00m 01s
–1641 Mar 17	13	–0.2772	1.0002	00m 01s
–0819 Jan 18	47	0.3047	1.0001	00m 00s
–0097 Mar 17	57	–0.5539	1.0001	00m 00s
0121 Dec 27	82	–0.6196	1.0002	00m 01s
0403 Nov 01	88	–0.1968	1.0001	00m 01s
1339 Jul 07	106	0.6451	1.0002	00m 01s
1612 Nov 22	136	–0.7691	1.0002	00m 01s
1627 Aug 11	139	0.9401	1.0001	00m 00s
1702 Jul 24	131	0.3160	1.0001	00m 01s
1804 Feb 11	137	0.7053	1.0000	00m 00s
1894 Apr 06	137	0.5740	1.0001	00m 01s
1986 Oct 03	124	0.9931	1.0000	00m 00s

Seven hybrid eclipses have a maximum magnitude (at greatest eclipse) greater than or equal to 1.0170. All of these events are central with a duration of totality of 1 min 34 s or more.

Table 3-19. Hybrid Eclipses with Magnitude 1.0170 or More

Date (Dynamical Time)	Saros	Gamma	Eclipse Magnitude	Central Duration
–0437 Dec 17	54	0.1286	1.0173	01m 45s
–0100 May 17	65	–0.1912	1.0170	01m 44s
0508 Sep 11	91	0.0826	1.0173	01m 45s
1199 Jan 28	108	0.0033	1.0174	01m 45s
1228 Jan 08	109	–0.0068	1.0176	01m 40s
1564 Jun 08	120	0.1253	1.0174	01m 44s
2172 Oct 17	146	–0.1484	1.0174	01m 34s

3.9 Greatest Central Duration—Annular Eclipses

Ten annular eclipses have a central duration (i.e., central line duration at greatest eclipse) of 12 min or more. There are no cases between the years 1974 and 3000.

Table 3-20. Annular Eclipses with Central Line Duration (at greatest eclipse) of 12 min or More

Date (Dynamical Time)	Saros	Gamma	Eclipse Magnitude	Central Duration
–1655 Dec 12	25	0.6207	0.9147	12m 07s
–0195 Dec 11	58	0.4971	0.9153	12m 04s
–0177 Dec 22	58	0.5030	0.9165	12m 08s
0132 Nov 25	83	0.5691	0.9144	12m 16s
0150 Dec 07	83	0.5630	0.9147	12m 23s
0168 Dec 17	83	0.5579	0.9156	12m 14s
1628 Dec 25	116	0.6265	0.9153	12m 02s
1937 Dec 02	141	0.4389	0.9184	12m 00s
1955 Dec 14	141	0.4266	0.9176	12m 09s
1973 Dec 24	141	0.4171	0.9174	12m 02s

3.10 Greatest Central Duration—Total Eclipses

Forty-four total eclipses have a central duration (i.e., central line duration at greatest eclipse) of seven minutes or more. These eclipses all take place when Earth is near the aphelion of its orbit (June to July), resulting in a smaller than normal diameter of the solar disk. The total eclipse with the longest duration of totality occurs on 2186 Jul 16. Its central duration of 7 min 29 s is very close to the theoretical maximum of 7 min 32.1 s during that epoch. All 44 eclipses belong to just 12 Saros series. Note that the eclipses of 1937, 1955, and 1973 all belong to Saros 136. This is the same Saros producing the 6+ min eclipses in 1991, 2009, and 2027.

Table 3-21. Total Eclipses with Central Line Duration (at greatest eclipse) of 7 min or More

Date (Dynamical Time)	Saros	Gamma	Eclipse Magnitude	Central Duration
–1460 Jun 22	23	–0.226	1.078	07m 04s
–1442 Jul 03	23	–0.293	1.076	07m 05s
–1124 May 28	29	–0.449	1.080	07m 03s
–1106 Jun 09	29	–0.524	1.079	07m 04s
–0779 May 24	54	–0.548	1.079	07m 12s
–0761 Jun 05	54	–0.474	1.080	07m 25s
–0743 Jun 15	54	–0.400	1.079	07m 28s
–0725 Jun 26	54	–0.329	1.078	07m 18s
–0707 Jul 07	54	–0.261	1.075	07m 00s
–0443 Apr 30	60	–0.319	1.077	07m 01s
–0425 May 12	60	–0.247	1.078	07m 12s
–0407 May 22	60	–0.173	1.078	07m 13s
–0389 Jun 02	60	–0.098	1.077	07m 04s
0114 May 22	78	–0.268	1.075	07m 06s
0132 Jun 01	78	–0.193	1.077	07m 14s
0150 Jun 12	78	–0.119	1.079	07m 13s
0168 Jun 23	78	–0.044	1.079	07m 03s
0327 Jun 06	81	–0.041	1.081	07m 03s
0345 Jun 16	81	–0.116	1.081	07m 17s
0363 Jun 27	81	–0.190	1.080	07m 24s
0381 Jul 08	81	–0.261	1.079	07m 22s
0399 Jul 19	81	–0.329	1.076	07m 11s
0681 May 23	87	–0.354	1.080	07m 10s
0699 Jun 03	87	–0.429	1.079	07m 17s
0717 Jun 13	87	–0.503	1.078	07m 15s
0735 Jun 25	87	–0.578	1.076	07m 02s
1044 May 29	112	–0.553	1.077	07m 12s
1062 Jun 09	112	–0.479	1.078	07m 20s
1080 Jun 20	112	–0.405	1.078	07m 18s
1098 Jul 01	112	–0.332	1.077	07m 05s
1937 Jun 08	136	–0.225	1.075	07m 04s
1955 Jun 20	136	–0.153	1.078	07m 08s
1973 Jun 30	136	–0.079	1.079	07m 04s
2150 Jun 25	139	–0.091	1.080	07m 14s
2168 Jul 05	139	–0.166	1.081	07m 26s
2186 Jul 16	139	–0.240	1.080	07m 29s
2204 Jul 27	139	–0.313	1.079	07m 22s
2222 Aug 08	139	–0.384	1.077	07m 06s
2504 Jun 14	145	–0.428	1.077	07m 10s
2522 Jun 25	145	–0.499	1.077	07m 12s
2540 Jul 05	145	–0.572	1.076	07m 04s
2867 Jun 23	170	–0.462	1.077	07m 10s
2885 Jul 03	170	–0.391	1.078	07m 11s
2903 Jul 16	170	–0.318	1.078	07m 04s

3.11 Greatest Central Duration—Hybrid Eclipses

Ten hybrid eclipses have a central duration (i.e., central line duration at greatest eclipse) greater than or equal to 1 min 40 s.

Table 3-22. Hybrid Eclipses with Central Line Duration (at greatest eclipse) of 1 min 40s or More

Date (Dynamical Time)	Saros	Gamma	Eclipse Magnitude	Central Duration
–1297 Sep 17	33	0.0674	1.0168	01m 40s
–0979 Aug 13	39	–0.2387	1.0168	01m 48s
–0437 Dec 17	54	0.1286	1.0173	01m 45s
–0100 May 17	65	–0.1912	1.0170	01m 44s
0508 Sep 11	91	0.0826	1.0173	01m 45s
1199 Jan 28	108	0.0033	1.0174	01m 45s
1228 Jan 08	109	–0.0068	1.0176	01m 40s
1350 Nov 30	112	0.2227	1.0166	01m 42s
1423 Jul 08	117	–0.1158	1.0161	01m 45s
1564 Jun 08	120	0.1253	1.0174	01m 44s

3.12 Theoretical Maximum Duration of Annularity

The theoretical maximum duration of an annular solar eclipse slowly varies because of long term secular changes in the eccentricity of Earth's orbit and the longitude of its perihelion. Although the maximum theoretical duration differs between the ascending and descending nodes, the durations are equal in the year +1246 because the Sun's perihelion then coincides with longitude 270°.

Table 3-23 lists the maximum duration theoretically possible over the period –2000 to +7000 (Meeus, 2007). The values here are 0.2 s smaller than those in Meeus because of the use of a slightly larger value for the Moon's radius *k* (Sect. 1.5).

Table 3-23. Theoretical Maximum Duration of Annularity

Year	Duration at Ascending Node	Duration at Descending Node
–2000	12m 16.8s	11m 40.9s
–1000	12m 30.2s	12m 04.8s
0000	12m 35.5s	12m 21.3s
+1000	12m 32.3s	12m 29.5s
+2000	12m 20.7s	12m 29.2s
+3000	12m 01.4s	12m 20.6s
+4000	11m 35.6s	12m 04.6s
+5000	11m 04.9s	11m 42.4s
+6000	10m 31.0s	11m 15.9s
+7000	10m 33.1s	11m 15.7s

The absolute maximum of 12 min 35.6 s occurred at the Moon's ascending node about the year +125. An inflexion point occurs between the years +6000 and +7000, when the maximum possible durations increase once again.

All calculations in the Canon use the same mean lunar radius "*k*" for both annular and total eclipses (Sect. 1.5). Consequently, the annular durations are extended several seconds because they include the appearance of Baily's beads[a] at the start and end of the antumbral phase.

3.13 Theoretical Maximum Duration of Totality

The theoretical maximum duration of a total solar eclipse for a point on Earth's surface slowly varies with time. This effect is due to long term secular changes in the eccentricity of Earth's orbit and the longitude of its perihelion. That eccentricity is now 0.01671, but at some epochs in the distant past or future the orbit was (will be) almost exactly circular, and at other times the eccentricity can be as large as 0.06.

Table 3-24 lists the maximum duration theoretically possible over the period –2000 to +7000 (Meeus 2003). The values here are 0.1 to 0.2 s larger than those in Meeus because of the use of a slightly larger value for the Moon's radius *k* (Sect. 1.5).

Table 3-24. Theoretical Maximum Duration of Totality

Year	Duration at Ascending Node	Duration at Descending Node
–2000	7m 07.4s	7m 29.8s
–1000	7m 19.1s	7m 34.6s
0000	7m 27.4s	7m 36.0s
+1000	7m 31.9s	7m 33.6s
+2000	7m 32.3s	7m 27.1s
+3000	7m 28.8s	7m 17.1s
+4000	7m 22.1s	7m 04.0s
+5000	7m 12.9s	6m 48.7s
+6000	7m 03.3s	6m 32.5s
+7000	7m 01.9s	6m 32.8s

The absolute maximum of 7 min 36.1 s occurred at the Moon's descending node about the year –120. Prior to –2000, there must have been epochs when the maximum possible duration was even larger due to an even greater value of the eccentricity of Earth's orbit.

3.14 Eclipse Duos

A duo is a pair of eclipses separated by one lunation (synodic month). Of the 11,898 eclipses in the *Canon*, 2,722eclipses (22.9%) belong to a duo. In most cases, both eclipses in a duo are partial eclipses, however, there are 14 instances in the *Canon* where one eclipse is partial and the other is total. The dates and eclipse combinations are listed in Table 3-25.

a. Baily's beads are caused by the appearance of small points of sunlight shining through deep valleys along the Moon's limb at the start and end of the annular or total phase.

Table 3-25. Eclipse Duos of Two Types

Dates (Dynamical Time)	Eclipse Combinations
–1859 May–Jun	TP
–1718 Apr–May	TP
–1310 May–Jun	PT
–1169 Apr–May	PT
–1028 Mar–Apr	PT
–0575 May–Jun	TP
–0434 Apr–May	TP
–0159 Jul–Aug	TP
–0026 May–Jun	PT
1248 May–Jun	TP
1928 May–Jun	TP
2195 Jul–Aug	PT
2459 May–Jun	PT
2912 Jul–Aug	TP

3.15 Eclipses Duos in One Calendar Month

There are 43 instances where both members of an eclipse duo occur in one calendar month. In all cases, both eclipses in the duos are partial. The year and month of each occurrence appears in Table 3-26.

Table 3-26. Two Eclipses in One Calendar Month

–1957 Mar	–1035 Aug	–0416 May	0629 Mar	2206 Dec
–1805 Jan	–1024 Jul	0007 Aug	1063 May	2261 Jan
–1610 Jul	–1013 Jun	0018 Jul	1150 Mar	2282 Nov
–1534 Jun	–0688 Dec	0097 Apr	1215 Mar	2304 Sep
–1523 May	–0677 Nov	0463 Aug	1631 May	2380 Aug
–1447 Apr	–0601 Oct	0528 Aug	1696 May	2684 Oct
–1209 Dec	–0590 Sep	0539 Jul	1805 Jan	2785 May
–1122 Oct	–0514 Aug	0542 May	1880 Dec	
–1111 Sep	–0503 Jul	0618 Apr	2000 Jul	

3.16 January–March Eclipse Duos

The mean length of one synodic month is 29.5306 days (in year 2000). Because this is longer than the month of February, it is possible to have one member of an eclipse duo in January followed by the second in March. There are four instances of such a rare January/March duo in the *Canon*: –1881, –1295, 1291, and 1794. In all cases, both eclipses in the duos are partial.

3.17 Eclipses on February 29

There are nine instances of a solar eclipse occurring on February 29. Five eclipses are partial, two are annular, and two are total. A list of eclipses on February 29 with physical parameters appears in Table 3-27.

Table 3-27. Eclipses on February 29

Date (Dynamical Time)	Type	Saros	Gamma	Eclipse Magnitude	Central Duration
–1436 Feb 29	P	7	–1.0586	0.9059	–
–0896 Feb 29	T	35	–0.3068	1.0652	05m 04s
–0356 Feb 29	T	63	0.4386	1.0628	05m 11s
0108 Feb 29	P	51	–1.5625	0.0082	–
0184 Feb 29	P	91	1.1684	0.6947	–
0648 Feb 29	A	79	–0.7722	0.9257	06m 44s
1188 Feb 29	A	107	0.0292	0.9294	08m 14s
2416 Feb 29	P	127	–1.4865	0.1279	–
2872 Feb 29	P	144	1.3315	0.3864	–

Section 4: Eclipse Periodicity

4.1 Interval Between Two Successive Eclipses

The time interval between any two successive solar eclipses can be either 1, 5, or 6 lunations (synodic months). The distribution of these 11,897 intervals in the *Canon* is found in Table 4-1.

Table 4-1. Interval Between Successive Eclipses

Number of Lunations	Number of Eclipses	Percent
1	1,361	11.4%
5	2,743	23.1%
6	7,793	65.5%

4.2 Saros Series

The periodicity and recurrence of eclipses can be investigated using the Saros cycle, a period of approximately 6,585.32 days (~18 years 11 days 8 hours). It was known to the Chaldeans as an interval when lunar eclipses appeared to repeat, but the Saros is applicable to solar eclipses as well.

The Saros arises from a harmonic between three of the Moon's orbital cycles. All three periods are subject to slow variations over long time scales, but their current values (2000 CE) are:

Synodic Month (New Moon to New Moon)	= 29.530589 days	= 29d 12h 44m
Draconic Month (node to node)	= 27.212221 days	= 27d 05h 06m
Anomalistic Month (perigee to perigee)	= 27.554550 days	= 27d 13h 19m

One Saros is equal to 223 synodic months, however, 242 draconic months and 239 anomalistic months are also equal (within a few hours) to this same period:

223 Synodic Months	= 6585.3223 days	= 6585d 07h 43m
242 Draconic Months	= 6585.3575 days	= 6585d 08h 35m
239 Anomalistic Months	= 6585.5375 days	= 6585d 12h 54m

Any two eclipses separated by one Saros cycle share similar characteristics. They occur at the same node with the Moon at nearly the same distance from Earth and at the same time of year. Because the Saros period is not equal to a whole number of days, its biggest drawback as an eclipse predictor is that subsequent eclipses are visible from different parts of the globe. The extra 1/3 day displacement means that Earth must rotate an additional ~8 hours or ~120° with each cycle. For solar eclipses, this results in a shift of each succeeding eclipse path by ~120° west. Thus, a Saros series returns to approximately the same geographic region every three Saros periods (~54 years and 34 days). This triple Saros cycle is known as the Exeligmos. Figure 4-1 shows the path of totality for nine eclipses belonging to Saros 136. This series is of particular interest because it is producing the longest total eclipses of the 20th and 21st centuries. The westward migration of each eclipse path from 1901 through 2045 illustrates the consequences of the extra 1/3 day in the Saros period. The northward shift of each path is due to the progressive increase in gamma from –0.3626 (1901) to 0.2116 (2045).

Figure 4-1 — Eclipses from Saros 136: 1901 to 2045

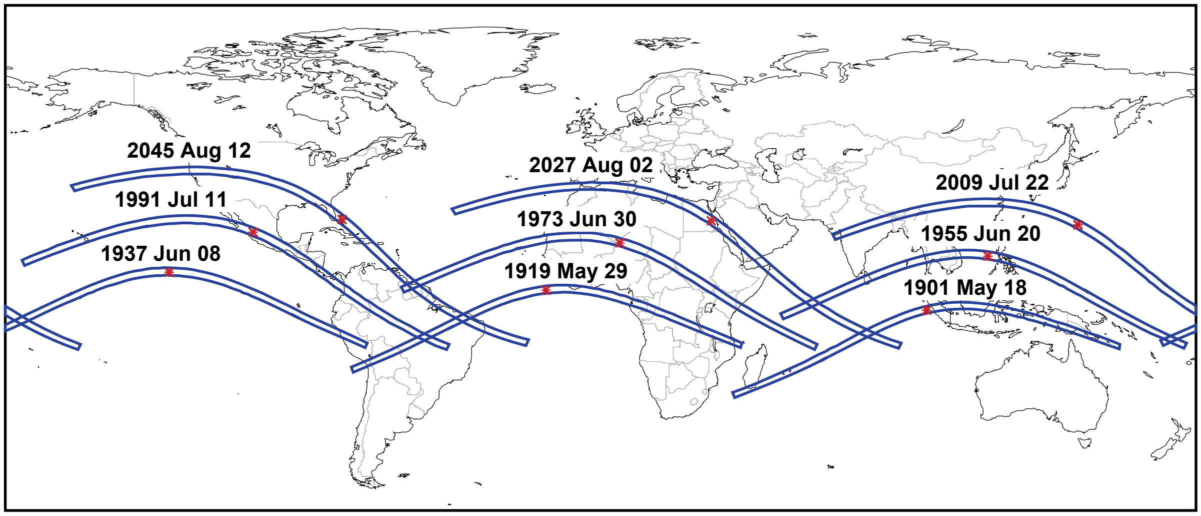

Saros series do not last indefinitely because the synodic, draconic, and anomalistic months are not perfectly commensurate with one another. In particular, the Moon's node shifts eastward by about 0.5° with each eclipse in a series. The following narrative describes the life cycle of a typical Saros series at the Moon's descending node. The series begins when the New Moon occurs ~17° east of the node. The Moon's umbral/antumbral shadow passes about 3500 km south of Earth and a small partial eclipse will be visible from high southern latitudes. One Saros period later, the umbra/antumbra passes ~250 km closer to Earth (gamma increases) and a partial eclipse of slightly larger magnitude will result. After about 10 Saros cycles (~200 years), the first umbral/antumbral eclipse occurs near the South Pole of Earth. Over the course of the next 7 to 10 centuries, a central eclipse occurs every 18.031 years (= Saros), but will be displaced northward by about 250 km with respect to Earth's center. Halfway through this period, eclipses of long duration occur near the equator (mid-series eclipses may be of short duration if hybrid or nearly so). The last central eclipse of the series takes place at high northern latitudes. Approximately 10 more eclipses will be partial with successively smaller magnitudes. Finally, the Saros series ends 12 to 15 centuries after it began at the opposite pole.

Based on the above description, the path of each umbral/antumbral eclipse should shift uniformly north in latitude after every Saros period. As Fig. 4-2 shows, this is not always the case. Nine members from Saros 136 are plotted for the years 2117 through 2261. Although the paths of previous eclipses in this series were shifting progressively northward (Figure 4-1), the trend here is reversed and the paths shift south. This temporary effect is due to the tilt of Earth's axis combined with the passage of Saros 136 eclipses from northern hemisphere autumnal equinox through winter solstice. Note that the season for this group of eclipses runs from September through December. With each successive eclipse, Earth's Northern Hemisphere tips further and further away from the Sun. This motion shifts geographic features and circles of latitude northward with respect to the Sun–Earth line at a rate that is faster than the change in gamma. Consequently, the eclipse paths appear to shift south in latitude until the winter solstice when they again resume a northward trend.

The scenario for a Saros series at the ascending node is similar except that gamma decreases as each successive eclipse shifts south of the previous one. The southern latitude trend in eclipse paths reverses to the north near the Northern Hemisphere summer solstice.

Because of the ellipticity of the orbits of Earth and the Moon, the exact duration and number of eclipses in a complete Saros series is not constant. A series may last 1,226 to 1,551 years and is composed of 69 to 87 eclipses, of which 39 to 59 are umbral/antumbral (i.e., annular, total, or hybrid). At present (2006), there are 39 active Saros series numbered 117 to 155. The number of eclipses in each of these series ranges from 70 to 82, however, the majority of the series (84.6%) are composed of 70 to 73 eclipses.

Figure 4-2 — Eclipses from Saros 136: 2117 to 2261

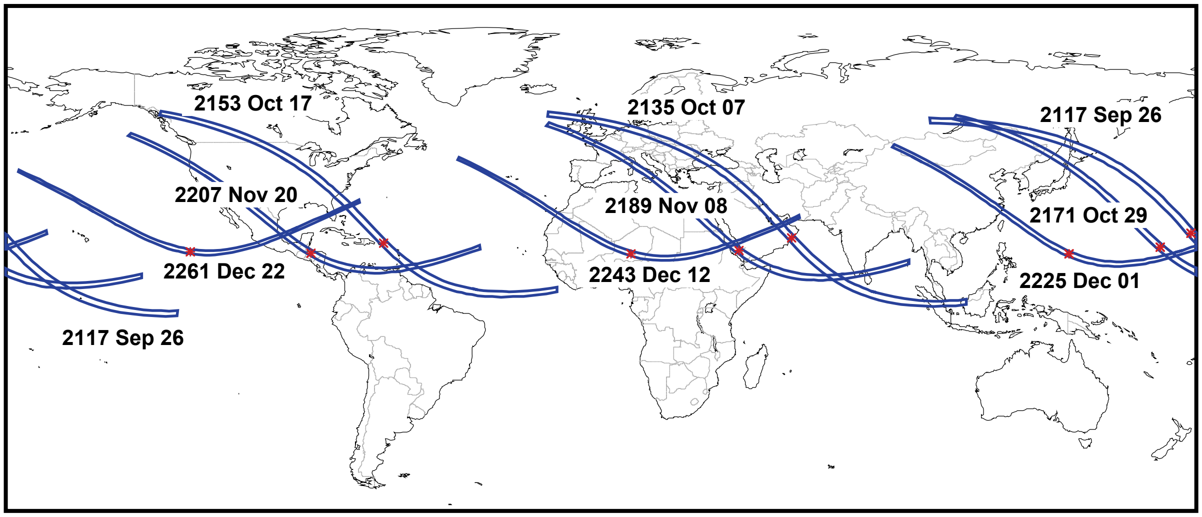

4.3 Gamma and Saros Series

Gamma changes monotonically throughout any single Saros series. As mentioned previously (Sect. 1.2.5), the change in gamma is larger when Earth is near its aphelion (June to July) than when it is near perihelion (December to January). For odd numbered series (ascending node), gamma decreases, while for even numbered series (descending node), gamma increases. This simple rule describes the current behavior of gamma, but this has not always been the case. The eccentricity of Earth's orbit is presently 0.0167, and is slowly decreasing. It was 0.0181 in the year –2000 and will be 0.0163 in +3000. In the past when the eccentricity was larger, there were Saros series in which the trend in gamma reversed for a few cycles before resuming its original direction. These instances occur near perihelion when the Sun's apparent motion is highest and may, in fact, overtake the eastward shift of the node. The resulting effect is a relative shift west of the node after one Saros cycle instead of the usual eastward shift. Consequently, gamma reverses direction.

The most unusual case of this occurs in Saros series 0. It began in –2955 with 11 partial eclipses, followed by 1 total, 1 hybrid, and 4 annulars. Gamma increased with each eclipse until it reversed direction with the second annular. It continued to decrease and the series began to once again produce partial eclipses. With the third partial eclipse, gamma resumed its original northward shift. The series went on to produce 45 more annular eclipses before ending in the year –1675 after 7 partial eclipses.

Among several hundred Saros series examined (–34 to 247), there are many other examples of temporary shifts in the monotonic nature of gamma, although none as bizarre as Saros 0. Some series have two separate reversals in gamma (e.g., series 15, 34, and 52) or even three (e.g., series –5 and 13). The most recent eclipse with a gamma reversal was in 1674 (Saros 107). The next and last in the *Canon* will occur in 2290 (Saros 165). In past millennia, the gamma reversals were more frequent because Earth's orbital eccentricity was larger.

4.4 Saros Series Statistics

Eclipses belonging to 204 different Saros series fall within the five millennium span of the *Canon*. Two series (–13 and 190) have only one or two members represented, while 81 have a larger but incomplete subset of their members included (–12 to –26, 30, 145, 147, and 151 to 189). Finally, 121 complete Saros series are contained within the *Canon* (27 to 29, 31 to 144, 146, and 148 to 150).

The number of eclipses in each of these series ranges from 69 to 87; however, over a quarter (27.9%) of the series contain 72 eclipses while nearly three quarters (72.1%) of them have 70 to 73 eclipses. Table 4-2 presents the statistical distribution of the number of eclipses in each Saros series. The approximate duration (years) as a function of the number of eclipses is listed along with the first five Saros series containing the corresponding number of eclipses.

Table 4-2. Number of Eclipses in Saros Series

Number of Eclipses	Duration (years)	Number of Series	Saros Series Numbers
69	1226	4	156, 171, 174, 177
70	1244	25	104, 116, 122, 123, 131,…
71	1262	40	22, 25, 61, 62, 64,…
72	1280	57	–11, 0, 1, 3, 4,…
73	1298	25	–13, –12, –3, 2, 5,…
74	1316	10	–8, –1, 9, 17, 31,…
75	1334	8	–10, –9, –2, 15, 74,…
76	1352	3	11, 108, 146
77	1370	3	145, 166, 184
78	1388	1	69
79	1406	2	111, 182
80	1424	4	–4, 129, 147, 164
81	1442	1	109
82	1460	2	71, 127
83	1478	4	30, 72, 88, 90
84	1496	5	32, 33, 35, 53, 70
85	1514	4	13, 14, 16, 51
86	1533	5	–7, –5, 12, 34, 52
87	1551	1	–6

All Saros series begin and end with a number of partial eclipses. Among the 204 Saros series with members falling within the scope of this *Canon*, the number of partial eclipses in the initial phase ranges from 6 to 25. Similarly, the number of partial eclipses in the final phase varies from 6 to 24. The middle life of a Saros series is composed of umbral/antumbral eclipses (i.e., annular, total, or hybrid), which range in number from 39 to 59. Table 4-3 presents the statistical distribution in the number of umbral/antumbral eclipses in the Saros series represented in the *Canon*.

Saros 0 is an exception to the above scheme. After beginning with 11 parial eclipses, Saros 0 proceeds with a total, a hybrid and an annular eclipse. The series then reverts back to 3 more partial eclipses. It finally resumes with a string of 45 annular eclipses before ending with 7 partial eclipses. This odd behavior is due to the higher eccentricity of the Moon’s orbit and fortuitous timing.

Table 4-3. Number of A/T/H Eclipses in Saros Series

Number of A/T/H Eclipses	Duration (years)	Number of Series	Saros Series Numbers
39	703	4	110, 144, 162, 165
40	721	19	–6, 31, 34, 37,…
41	739	21	–9, –3, 12, 13,…
42	757	17	10, 15, 16, 28,…
43	775	30	–8, –7, –5, –4,…
44	793	18	–2, 11, 17, 18,…
45	811	7	–12, 29, 48, 77,…
46	829	3	–10, 114, 151
47	847	1	140
48	865	5	–1, 38, 66, 171, 188
49	883	2	27, 153
50	902	1	103
51	920 [a]	2	0, 190
52	938	4	57, 64, 156, 189
53	956	8	40, 101, 116, 133,…
54	974	6	47, 98, 119, 134,…
55	992	14	43, 59, 82, 83,…
56	1010	17	–11, 1, 6, 8,…
57	1028	13	3, 4, 7, 20,…
58	1046	10	–13, 2, 21, 26,…
59	1064	2	5, 23

a. The duration of the A/T/H eclipse sequence of Saros 0 is 974 years because it contains 3 partial eclipses.

A concise summary of all 204 Saros series (–13 to 190) is presented in Tables 4-4 to 4-9. The number of eclipses in each series is listed followed by the calendar dates of the first and last eclipses in the Saros. Finally, the chronological sequence of eclipse types in the series is tabulated. The number and type of eclipses varies from one Saros series to the next as reflected in the sequence diversity. Note that the tables make no distinction between central and non-central umbral/antumbral eclipses. The following abbreviations are used in the eclipse sequences:

P = Partial Eclipse
A = Annular Eclipse
T = Total Eclipse
H = Hybrid Eclipse

Table 4-4. Summary of Saros Series –13 to 23

Saros Series	Number of Eclipses	First Eclipse	Last Eclipse	Eclipse Sequence
–13	73	–3277 Mar 15	–1979 May 02	7P 39T 2H 17A 8P
–12	73	–3230 Mar 06	–1932 Apr 22	8P 1T 2H 42A 20P
–11	72	–3147 Mar 17	–1867 Apr 24	6P 24A 3H 29T 10P
–10	75	–3172 Jan 24	–1838 Apr 04	9P 40T 2H 4A 20P
–9	75	–3125 Jan 15	–1791 Mar 25	10P 1T 2H 38A 24P
–8	74	–3042 Jan 27	–1726 Mar 27	8P 25A 3H 15T 23P
–7	86	–3248 Aug 18	–1715 Feb 24	21P 41T 1H 1A 22P
–6	87	–3237 Jul 19	–1686 Feb 03	25P 3H 37A 22P
–5	86	–3136 Aug 10	–1603 Feb 16	21P 26A 3H 14T 22P
–4	80	–3143 Jun 29	–1719 Nov 01	23P 41T 1H 1A 14P
–3	73	–3096 Jun 20	–1798 Aug 07	24P 41A 8P
–2	75	–3013 Jul 03	–1679 Sep 10	21P 27A 4H 13T 10P
–1	74	–3002 Jun 01	–1686 Jul 31	18P 44T 3H 1A 8P
0	72	–2955 May 23	–1675 Jun 29	11P 1T 1H 4A 3P 45A 7P
1	72	–2872 Jun 04	–1592 Jul 11	9P 39A 5H 12T 7P
2	73	–2861 May 04	–1563 Jun 21	8P 43T 12H 3A 7P
3	72	–2814 Apr 24	–1534 Jun 01	8P 5T 2H 50A 7P
4	72	–2731 May 06	–1451 Jun 13	7P 29A 17H 11T 8P
5	73	–2720 Apr 04	–1422 May 24	7P 44T 4H 11A 7P
6	72	–2673 Mar 27	–1393 May 03	7P 7T 2H 47A 9P
7	72	–2590 Apr 08	–1310 May 16	6P 30A 6H 21T 9P
8	73	–2579 Mar 07	–1281 Apr 26	7P 45T 1H 10A 10P
9	74	–2568 Feb 06	–1252 Apr 04	9P 8T 3H 32A 22P
10	73	–2467 Feb 28	–1169 Apr 18	8P 30A 3H 9T 23P
11	76	–2492 Jan 06	–1140 Mar 28	10P 44T 22P
12	86	–2662 Aug 20	–1129 Feb 25	23P 8T 3H 30A 22P
13	85	–2543 Sep 23	–1028 Mar 19	20P 30A 3H 8T 24P
14	85	–2550 Aug 11	–1035 Feb 06	21P 43T 21P
15	75	–2557 Jul 01	–1223 Sep 08	24P 10T 3H 29A 9P
16	85	–2456 Jul 23	–0941 Jan 18	22P 33A 2H 7T 21P
17	74	–2427 Jul 03	–1111 Sep 01	21P 44T 9P
18	73	–2416 Jun 02	–1118 Jul 21	22P 13T 3H 28A 7P
19	73	–2333 Jun 15	–1035 Aug 01	21P 36A 2H 6T 8P
20	72	–2286 Jun 05	–1006 Jul 13	8P 12A 2H 43T 7P
21	72	–2275 May 05	–0995 Jun 11	8P 26T 4H 28A 6P
22	71	–2174 May 28	–0912 Jun 23	8P 49A 2H 5T 7P
23	72	–2145 May 07	–0865 Jun 15	6P 14A 3H 42T 7P

Table 4-5. Summary of Saros Series 24 to 60

Saros Series	Number of Eclipses	First Eclipse	Last Eclipse	Eclipse Sequence
24	72	–2134 Apr 06	–0854 May 14	8P 15T 16H 26A 7P
25	71	–2033 Apr 30	–0771 May 26	7P 52A 1H 3T 8P
26	72	–2004 Apr 08	–0724 May 17	6P 10A 7H 41T 8P
27	72	–1993 Mar 09	–0713 Apr 16	8P 14T 15H 20A 15P
28	72	–1910 Mar 22	–0630 Apr 28	7P 42A 23P
29	73	–1881 Mar 01	–0583 Apr 19	7P 3A 14H 28T 21P
30	83	–2051 Oct 12	–0572 Mar 18	19P 14T 5H 24A 21P
31	74	–1805 Jan 31	–0489 Mar 31	10P 40A 24P
32	84	–1957 Sep 24	–0460 Mar 10	19P 2A 3H 39T 21P
33	84	–1982 Aug 02	–0485 Jan 17	23P 15T 4H 23A 19P
34	86	–1917 Aug 04	–0384 Feb 09	23P 40A 23P
35	84	–1870 Jul 25	–0373 Jan 09	22P 3A 2H 38T 19P
36	73	–1859 Jun 23	–0561 Aug 11	22P 18T 3H 23A 7P
37	73	–1794 Jun 25	–0496 Aug 12	24P 40A 9P
38	73	–1729 Jun 26	–0431 Aug 14	17P 8A 2H 38T 8P
39	72	–1718 May 26	–0438 Jul 03	9P 32T 3H 22A 6P
40	72	–1653 May 28	–0373 Jul 04	11P 53A 8P
41	72	–1588 May 28	–0308 Jul 05	7P 19A 2H 37T 7P
42	72	–1577 Apr 28	–0297 Jun 05	8P 34T 3H 21A 6P
43	72	–1512 Apr 29	–0232 Jun 05	8P 55A 9P
44	72	–1447 Apr 30	–0167 Jun 07	6P 21A 2H 35T 8P
45	72	–1436 Mar 30	–0156 May 07	7P 36T 3H 18A 8P
46	72	–1371 Apr 01	–0091 May 08	8P 43A 21P
47	72	–1306 Apr 02	–0026 May 10	6P 21A 3H 30T 12P
48	74	–1331 Feb 08	–0015 Apr 09	9P 37T 2H 6A 20P
49	72	–1248 Feb 22	0032 Mar 29	9P 40A 23P
50	73	–1201 Feb 11	0097 Apr 01	8P 22A 3H 18T 22P
51	85	–1407 Sep 02	0108 Feb 29	21P 36T 4H 3A 21P
52	86	–1378 Aug 14	0155 Feb 19	24P 40A 22P
53	84	–1277 Sep 06	0220 Feb 21	20P 22A 4H 17T 21P
54	74	–1284 Jul 25	0032 Sep 23	21P 26T 15H 3A 9P
55	73	–1255 Jul 06	0043 Aug 23	24P 41A 8P
56	74	–1172 Jul 17	0144 Sep 15	21P 13A 15H 15T 10P
57	73	–1161 Jun 17	0137 Aug 04	14P 33T 13H 6A 7P
58	72	–1114 Jun 07	0166 Jul 14	21P 44A 7P
59	72	–1031 Jun 19	0249 Jul 27	9P 23A 16H 16T 8P
60	72	–1020 May 18	0260 Jun 26	8P 40T 4H 14A 6P

Table 4-6. Summary of Saros Series 61 to 97

Saros Series	Number of Eclipses	First Eclipse	Last Eclipse	Eclipse Sequence
61	71	–0973 May 10	0289 Jun 05	8P 3T 1H 52A 7P
62	71	–0890 May 22	0372 Jun 17	7P 25A 5H 27T 7P
63	72	–0879 Apr 20	0401 May 29	7P 42T 2H 14A 7P
64	71	–0832 Apr 11	0430 May 08	8P 4T 2H 46A 11P
65	71	–0749 Apr 24	0513 May 20	6P 27A 4H 25T 9P
66	73	–0756 Mar 12	0542 May 01	8P 43T 1H 4A 17P
67	72	–0709 Mar 04	0571 Apr 10	9P 5T 2H 34A 22P
68	72	–0626 Mar 16	0654 Apr 22	7P 28A 3H 11T 23P
69	78	–0724 Dec 09	0665 Mar 22	14P 43T 21P
70	84	–0821 Sep 05	0676 Feb 19	23P 5T 3H 32A 21P
71	82	–0684 Oct 19	0777 Mar 14	18P 29A 3H 9T 23P
72	83	–0727 Aug 16	0752 Jan 21	22P 43T 18P
73	72	–0698 Jul 27	0582 Sep 03	23P 7T 3H 31A 8P
74	75	–0615 Aug 08	0719 Oct 18	22P 30A 3H 8T 12P
75	73	–0604 Jul 07	0694 Aug 26	21P 44T 8P
76	72	–0575 Jun 18	0705 Jul 25	22P 8T 5H 30A 7P
77	71	–0474 Jul 11	0788 Aug 06	18P 36A 2H 7T 8P
78	72	–0463 Jun 09	0817 Jul 18	9P 9A 2H 45T 7P
79	71	–0434 May 21	0828 Jun 16	8P 11T 16H 30A 6P
80	71	–0333 Jun 13	0929 Jul 09	7P 48A 2H 6T 8P
81	72	–0322 May 12	0958 Jun 19	7P 5A 9H 44T 7P
82	71	–0293 Apr 22	0969 May 19	8P 11T 5H 39A 8P
83	71	–0210 May 05	1052 May 30	7P 51A 1H 3T 9P
84	72	–0181 Apr 14	1099 May 22	7P 1A 11H 43T 10P
85	72	–0170 Mar 14	1110 Apr 20	8P 12T 4H 29A 19P
86	71	–0069 Apr 06	1193 May 02	7P 41A 23P
87	73	–0076 Feb 23	1222 Apr 13	9P 2H 42T 20P
88	83	–0246 Oct 06	1233 Mar 12	20P 13T 4H 26A 20P
89	73	0018 Feb 04	1316 Mar 24	10P 40A 23P
90	83	–0134 Sep 28	1345 Mar 04	20P 2H 40T 21P
91	75	–0159 Aug 06	1175 Oct 16	23P 14T 3H 25A 10P
92	74	–0076 Aug 19	1240 Oct 16	23P 40A 11P
93	74	–0029 Aug 09	1287 Oct 08	20P 3A 1H 40T 10P
94	72	–0018 Jul 09	1262 Aug 16	21P 18T 2H 24A 7P
95	71	0047 Jul 11	1309 Aug 06	22P 41A 8P
96	72	0094 Jul 01	1374 Aug 08	10P 14A 2H 39T 7P
97	71	0123 Jun 11	1385 Jul 08	8P 32T 2H 23A 6P

Table 4-7. Summary of Saros Series 98 to 134

Saros Series	Number of Eclipses	First Eclipse	Last Eclipse	Eclipse Sequence
98	71	0188 Jun 12	1450 Jul 09	9P 54A 8P
99	72	0235 Jun 03	1515 Jul 11	7P 18A 2H 37T 8P
100	71	0264 May 13	1526 Jun 10	7P 34T 2H 21A 7P
101	71	0329 May 15	1591 Jun 21	8P 53A 10P
102	71	0376 May 05	1638 Jun 12	7P 19A 3H 34T 8P
103	72	0387 Apr 04	1667 May 22	8P 34T 3H 13A 14P
104	70	0470 Apr 17	1714 May 13	7P 41A 22P
105	72	0499 Mar 27	1779 May 16	7P 20A 4H 21T 20P
106	75	0456 Jan 23	1790 Apr 14	12P 34T 4H 5A 20P
107	72	0557 Feb 15	1837 Apr 05	10P 40A 22P
108	76	0550 Jan 04	1902 Apr 08	12P 20A 5H 18T 21P
109	81	0416 Sep 07	1859 Feb 03	21P 24T 15H 4A 17P
110	72	0463 Aug 30	1743 Oct 17	23P 39A 10P
111	79	0528 Aug 30	1935 Jan 05	21P 11A 14H 17T 16P
112	72	0539 Jul 31	1819 Sep 19	21P 24T 14H 5A 8P
113	71	0586 Jul 22	1848 Aug 28	23P 40A 8P
114	72	0651 Jul 23	1931 Sep 12	18P 13A 16H 17T 8P
115	72	0662 Jun 21	1942 Aug 12	10P 37T 4H 14A 7P
116	70	0727 Jun 23	1971 Jul 22	10P 53A 7P
117	71	0792 Jun 24	2054 Aug 03	8P 23A 5H 28T 7P
118	72	0803 May 24	2083 Jul 15	8P 40T 2H 15A 7P
119	71	0850 May 15	2112 Jun 24	8P 2T 1H 51A 9P
120	71	0933 May 27	2195 Jul 07	7P 25A 4H 26T 9P
121	71	0944 Apr 25	2206 Jun 07	7P 42T 2H 11A 9P
122	70	0991 Apr 17	2235 May 17	8P 3T 2H 37A 20P
123	70	1074 Apr 29	2318 May 31	6P 27A 3H 14T 20P
124	73	1049 Mar 06	2347 May 11	9P 43T 1H 20P
125	73	1060 Feb 04	2358 Apr 09	12P 4T 2H 34A 21P
126	72	1179 Mar 10	2459 May 03	8P 28A 3H 10T 23P
127	82	0991 Oct 10	2452 Mar 21	20P 42T 20P
128	73	0984 Aug 29	2282 Nov 01	24P 4T 4H 32A 9P
129	80	1103 Oct 03	2528 Feb 21	20P 29A 3H 9T 19P
130	73	1096 Aug 20	2394 Oct 25	21P 43T 9P
131	70	1125 Aug 01	2369 Sep 02	22P 6T 5H 30A 7P
132	71	1208 Aug 13	2470 Sep 25	20P 33A 2H 7T 9P
133	72	1219 Jul 13	2499 Sep 05	12P 6A 1H 46T 7P
134	71	1248 Jun 22	2510 Aug 06	10P 8T 16H 30A 7P

Table 4-8. Summary of Saros Series 135 to 171

Saros Series	Number of Eclipses	First Eclipse	Last Eclipse	Eclipse Sequence
135	71	1331 Jul 05	2593 Aug 17	10P 45A 2H 6T 8P
136	71	1360 Jun 14	2622 Jul 30	8P 6A 6H 44T 7P
137	70	1389 May 25	2633 Jun 28	8P 10T 6H 4A 3H 32A 7P
138	70	1472 Jun 06	2716 Jul 11	7P 50A 1H 3T 9P
139	71	1501 May 17	2763 Jul 03	7P 12H 43T 9P
140	71	1512 Apr 16	2774 Jun 01	8P 11T 4H 32A 16P
141	70	1613 May 19	2857 Jun 13	7P 41A 22P
142	72	1624 Apr 17	2904 Jun 05	8P 1H 43T 20P
143	72	1617 Mar 07	2897 Apr 23	10P 12T 4H 26A 20P
144	70	1736 Apr 11	2980 May 05	8P 39A 23P
145	77	1639 Jan 04	3009 Apr 17	14P 1A 1H 41T 20P
146	76	1541 Sep 19	2893 Dec 29	22P 13T 4H 24A 13P
147	80	1624 Oct 12	3049 Feb 24	21P 40A 19P
148	75	1653 Sep 21	2987 Dec 12	20P 2A 1H 40T 12P
149	71	1664 Aug 21	2926 Sep 28	21P 17T 3H 23A 7P
150	71	1729 Aug 24	2991 Sep 29	22P 40A 9P
151	72	1776 Aug 14	3056 Oct 01	18P 6A 1H 39T 8P
152	70	1805 Jul 26	3049 Aug 20	9P 30T 3H 22A 6P
153	70	1870 Jul 28	3114 Aug 22	13P 49A 8P
154	71	1917 Jul 19	3179 Aug 25	7P 17A 3H 36T 8P
155	71	1928 Jun 17	3190 Jul 24	8P 33T 3H 20A 7P
156	69	2011 Jul 01	3237 Jul 14	8P 52A 9P
157	70	2058 Jun 21	3302 Jul 17	6P 19A 3H 34T 8P
158	70	2069 May 20	3313 Jun 16	7P 35T 2H 16A 10P
159	70	2134 May 23	3378 Jun 17	8P 41A 21P
160	71	2181 May 13	3443 Jun 20	7P 20A 3H 22T 19P
161	72	2174 Apr 01	3454 May 20	9P 35T 3H 5A 20P
162	70	2257 Apr 15	3501 May 10	9P 39A 22P
163	72	2286 Mar 25	3566 May 13	9P 20A 4H 18T 21P
164	80	2098 Oct 24	3523 Mar 10	20P 36T 4H 3A 17P
165	72	2145 Oct 16	3425 Dec 02	22P 39A 11P
166	77	2228 Oct 29	3599 Feb 08	19P 21A 5H 16T 16P
167	72	2203 Sep 06	3483 Oct 24	21P 26T 14H 3A 8P
168	70	2250 Aug 28	3494 Sep 22	23P 40A 7P
169	71	2333 Sep 10	3595 Oct 16	19P 13A 16H 15T 8P
170	71	2344 Aug 09	3606 Sep 15	11P 36T 11H 6A 7P
171	69	2391 Aug 01	3617 Aug 14	14P 48A 7P

Table 4-9. Summary of Saros Series 172 to 190

Saros Series	Number of Eclipses	First Eclipse	Last Eclipse	Eclipse Sequence
172	70	2474 Aug 13	3718 Sep 08	8P 23A 16H 15T 8P
173	70	2485 Jul 12	3729 Aug 08	7P 41T 3H 12A 7P
174	69	2532 Jul 04	3758 Jul 18	8P 1T 2H 50A 8P
175	70	2597 Jul 05	3841 Jul 31	7P 26A 5H 24T 8P
176	71	2608 Jun 04	3870 Jul 12	7P 43T 2H 10A 9P
177	69	2655 May 27	3881 Jun 10	8P 3T 3H 37A 18P
178	70	2738 Jun 09	3982 Jul 04	6P 28A 4H 11T 21P
179	71	2731 Apr 28	3993 Jun 03	8P 44T 19P
180	70	2760 Apr 08	4004 May 02	10P 5T 2H 33A 20P
181	71	2843 Apr 20	4105 May 27	8P 29A 3H 9T 22P
182	79	2691 Dec 11	4098 Apr 15	18P 42T 19P
183	72	2666 Oct 20	3946 Dec 06	22P 6T 4H 30A 10P
184	77	2785 Nov 24	4156 Mar 05	19P 30A 3H 7T 18P
185	73	2760 Oct 01	4058 Nov 29	21P 42T 10P
186	70	2789 Sep 11	4033 Oct 06	22P 8T 4H 29A 7P
187	70	2872 Sep 23	4116 Oct 19	20P 34A 2H 5T 9P
188	71	2883 Aug 23	4145 Sep 30	16P 3A 1H 44T 7P
189	70	2912 Aug 04	4156 Aug 29	11P 19T 6H 27A 7P
190	70	2995 Aug 17	4239 Sep 12	11P 46A 2H 3T 8P

4.5 Saros and Other Periods

The numbering system used for the Saros series was introduced by van den Bergh in his book *Periodicity and Variation of Solar (and Lunar) Eclipses* (1955). He assigned the number 1 to a pair of solar and lunar eclipse series that were in progress during the second millennium BCE based on an extrapolation from Oppolzer's *Canon der Finsternisse* (1887).

There is an interval of 1, 5, or 6 synodic months between any sequential pair of solar eclipses. Interestingly, the number of lunations between two eclipses permits the determination of the Saros series number of the second eclipse when the Saros series number of the first eclipse is known. Let the Saros series number of the first eclipse in a pair be "s". The Saros series number of the second eclipse can be found from the relationships in Table 4-10 (Meeus, Grosjean, and Vanderleen, 1966).

Table 4-10. Some Eclipse Periods and Their Relationships to the Saros Number

Number of Synodic Months	Length of Time	Saros Series Number	Period Name
1	~1 month	s + 38	Lunation
5	~5 months	s – 33	Short Semester
6	~6 months	s + 5	Semester
135	~11 years – 1 month	s + 1	Tritos
223	~18 years + 11 days	s	Saros
235	~19 years	s + 10	Metonic Cycle
358	~29 years – 20 days	s + 1	Inex
669	~54 years + 33 days	s	Exeligmos (Triple Saros)

4.6 Saros and Inex

A number of different eclipse cycles were investigated by van den Bergh, but the most useful were the Saros and the Inex. The Inex is equal to 358 synodic months (~29 years less 20 days), which is very nearly 388.5 draconic months.

358 Synodic Months	= 10,571.9509 days	= 10,571d 22h 49m
388.5 Draconic Months	= 10,571.9479 days	= 10,571d 22h 55m

The extra 0.5 in the number of draconic months means that eclipses separated by one Inex period occur at opposite nodes. Consequently, an eclipse visible from the Northern Hemisphere will be followed one Inex later by an eclipse visible from the Southern Hemisphere, and vice versa. The Inex is equal to ~383.67 anomalistic months, which is far from an integer number. Thus, eclipses separated by one Inex will very likely be of different types, especially if they are central (i.e., total or annular).

The mean time difference between 358 synodic months and 388.5 draconic months making up an Inex is only 6 min. In comparison, the mean difference between these two cycles in the Saros is 52 min. This means that after one Inex, the shift of the Moon with respect to the node (+0.04°) is much smaller than for the Saros (–0.48°). While a Saros series lasts 12 to 15 centuries, an Inex series typically lasts 225 centuries and contains about 780 eclipses. Although the Inex posesses a long lifespan, its mean duration is not easily characterized because the length of the synodic and draconic months are changing over long time scales. If the instantaneous mean durations of the synodic and draconic months for the years –2000, +2000, and +4000 are used to calculate the mean duration of the Inex, the resulting lengths are about 14,500, 26,600, and 51,000 years, respectively (Meeus, 2004).

Van den Bergh placed all 8,000 solar eclipses in Oppolzer's *Canon der Finsternisse* (1887) into a large two-dimensional matrix. Each Saros series was arranged as a separate column containing every eclipse in chronological order. The individual Saros columns were then staggered so that the horizontal rows each corresponded to different Inex series. This "Saros–Inex Panorama" proved useful in organizing eclipses. For instance, one step down in the panorama is a change of one Saros period (6585.32 days) later, while one step to the right is a change of one Inex period (10571.95 days) later. The rows and columns were then numbered with the Saros and Inex numbers.

The panorama also made it possible to predict the approximate circumstances of solar (and lunar) eclipses occurring before or after the period spanned by Oppolzer's *Canon*. The time interval "*t*" between any two solar eclipses can be found through an integer combination of Saros and Inex periods via the following relationship:

$$t = a\,i + b\,s, \qquad (29)$$

where

t = interval in days,
i = Inex period of 10571.95 days (358 synodic months),
s = Saros period of 6585.32 days (223 synodic months), and
a, b = integers (negative, zero, or positive).

From this equation, a number of useful combinations of Inex and Saros periods can be employed to extend Oppolzer's *Canon* from –1207 back to –1600 using nothing more than simple arithmetic (van den Bergh, 1954). The ultimate goal of the effort was to a produce an eclipse canon for dating historical events prior to –1207. Periods formed by various combinations of Inex and Saros were evaluated in order to satisfy one or more of the following conditions:

1) The deviation from a multiple of 0.5 draconic months should be small (i.e., Moon should be nearly the same distance from the node).
2) The deviation from an integral multiple of anomalistic months should be small (i.e., Moon should be nearly the same distance from Earth).
3) The deviation from an integral multiple of anomalistic years should be small (i.e., eclipse should occur on nearly the same calendar date).

No single Inex–Saros combination meets all three criteria, but there are periods that do a reasonably good job for any one of them. Note that secular changes in the Moon's elements cause a particular period to be of high accuracy for a limited number of centuries. The direct application of the Saros–Inex panorama allows for the determination of eclipse dates in the past (or future); however, the application of the longer Saros–Inex combinations permit the rapid estimation of a number of eclipse characteristics without lengthy calculations. Table 4-11 lists several of the most useful periods.

Table 4-11. Some Useful Eclipse Periods

Period Name	Period (Inex + Saros)	Period (years)	Use
Heliotrope	$58i + 6s$	1,787	Geographic longitude of central line
Accuratissima	$58i + 9s$	1,841	Geographic latitude of central line
Horologia	$110i + 7s$	3,310	Time of ecliptic conjunction

Modern digital computers using high precision solar and lunar ephemerides can directly predict the dates and circumstances of eclipses. Nevertheless, the Saros and Inex cycles are still of great value in understanding the periodicity and frequency of eclipses.

ABBREVIATIONS

arcsec	Arc second
AT	Hybrid eclipse that begins as annular, then changes to total.
ATA	Hybrid eclipse that begins as annular, changes to total, and then reverts back to annular.
BCE	Before the Common Era
CE	Common Era
cm	Centimeter
ET	Ephemeris Time
GMAT	Greenwich Mean Astronomical Time
GMT	Greenwich Mean Time
IAU	International Astronomical Union
ISO	International Standards Organization
LLR	Lunar Laser Ranging
LOD	Length of Day
m	Meter (or minutes in tables)
min	Minutes
s	Second
arcsec/cy^2	Arc seconds per Julian century squared
TA	Hybrid eclipse that begins as total and ends as annular.
TAI	International Atomic Time
TD	Terrestrial Dynamical Time
TT	Terrestrial Time
UT	Universal Time
UTC	Coordinated Universal Time
VLBI	Very Long Baseline Interferometry

References

Astronomical Almanac for 2006, Washington: US Government Printing Office; London: HM Stationery Office (2004).

Bretagnon P., Francou G., "Planetary theories in rectangular and spherical variables: VSOP87 solution," *Astron. Astrophys.,* **202**(309) (1988).

Brown, E.W., "Theory of the Motion of the Moon," *Mem. Royal Astron. Soc.,* Vol. LVII, Part II, pp. 136–141, London (1905).

Chapront-Touzé, M., and Chapront, J., "The Lunar Ephemeris ELP 2000," *Astron. Astrophys.,* vol. 124, no. 1, pp. 50–62 (1983).

Chapront, J., Chapront-Touzé, M., and Francou, G., "A new determination of lunar orbital parameters, precession constant and tidal acceleration from LLR measurements," *Astron. Astrophys.,* vol. 387, pp. 700–709 (2002).

Dickey, J.O., et al. , "Lunar Laser Ranging: a Continuing Legacy of the Apollo Program," *Science*, 265, pp. 482–490 (1994).

Espenak, F., *Fifty Year Canon of Solar Eclipses: 1986–2035*, NASA RP-1178, Sky Publishing Corp., Cambridge (1987).

Explanatory Supplement to the Ephemeris, H.M. Almanac Office, London (1974).

Ginzel, F.K., *Spezieller Kanon der Sonnen- und Mondfinsternisse*, Berlin (1899).

Huber, P.J., "Modeling the Length of Day and Extrapolating the Rotation of the Earth," *Astronomical Amusements*, F. Bònoli, S. De Meis, and A. Panaino, Eds., Rome (2000).

Improved Lunar Ephemeris 1952–1959, Nautical Almanac Office, U.S. Naval Observatory, Washington, DC (1954).

Meeus, J., *Mathematical Astronomy Morsels*, Willmann-Bell, pp. 56–62 (1997).

——, *More Mathematical Astronomy Morsels*, Willmann-Bell, pp. 120–126 (2002).

——, "The maximum possible duration of a total solar eclipse," *J. Br. Astron. Assoc.,* **113**(6) (2003).

——, *Mathematical Astronomy Morsels III*, Willmann-Bell, pp. 109–111, (2004).

——, *Mathematical Astronomy Morsels IV*, Willmann-Bell, in preparation (~2007).

——, Grosjean, C.C., and Vanderleen, W., *Canon of Solar Eclipses*, Pergamon Press, Oxford (1966).

Morrison, L., and Stephenson, F.R., "Historical Values of the Earth's Clock Error ΔT and the Calculation of Eclipses," *J. Hist. Astron.,* Vol. 35 Part 3, August 2004, No. 120, pp, 327–336 (2004).

Mucke, H., and Meeus, J., *Canon of Solar Eclipses: –2003 to +2526*, Astronomisches Büro, Vienna (1983).

Newcomb, S., "Tables of the Motion of the Earth on its Axis Around the Sun,", *Astron. Papers Amer. Eph.,* Vol. 6, Part I (1895).

Oppolzer, T.R. von, *Canon der Finsternisse*, Wien, (1887).

Reprinted: *Canon of Eclipses*, Translated by O. Gingerich, Dover Publications, New York (1962).

Schroeter, J. Fr., *Sonnenfinsternisse von 600 bis 1800 n. Chr.*, Kristiania (1923).

Stephenson, F.R., *Historical Eclipses and Earth's Rotation*, Cambridge University Press, Cambridge (1997).

——, and Houlden, M.A., *Atlas of Historical Eclipse Maps, East Asia 1500BC—AD 1900*, Cambridge University Press, Cambridge/New York (1986).

van den Bergh, *Eclipses in the Second Millennium B.C. –1600 to –1207*, Tjeenk Willink, and Haarlem, Netherlands (1954).

——, *Periodicity and Variation of Solar (and Lunar) Eclipses*, Tjeenk Willink, and Haarlem, Netherlands (1955).